

Review

## Recent Progress on Fe/N/C Electrocatalysts for the Oxygen Reduction Reaction in Fuel Cells

Jing Liu <sup>1,2</sup>, Erling Li <sup>1,2,3</sup>, Mingbo Ruan <sup>1,2</sup>, Ping Song <sup>1,2</sup> and Weilin Xu <sup>1,2,\*</sup>

<sup>1</sup> State Key Laboratory of Electroanalytical Chemistry, Changchun Institute of Applied Chemistry, Chinese Academy of Science, 5625 Renmin Street, Changchun 130022, China;

E-Mails: liujing@ciac.ac.cn (J.L.); lingli2013@ciac.ac.cn (E.L.); ruanmb@ciac.ac.cn (M.R.); songping@ciac.ac.cn (P.S.)

<sup>2</sup> Jilin Province Key Laboratory of Low Carbon Chemical Power, Changchun Institute of Applied Chemistry, Chinese Academy of Science, 5625 Renmin Street, Changchun 130022, China

<sup>3</sup> Graduate University of Chinese Academy of Science, Beijing 100049, China

\* Author to whom correspondence should be addressed; E-Mail: weilinxu@ciac.ac.cn; Tel./Fax: +86-0431-85262848.

Academic Editor: Minhua Shao

Received: 11 May 2015 / Accepted: 23 June 2015 / Published: 6 July 2015

---

**Abstract:** In order to reduce the overall system cost, the development of inexpensive, high-performance and durable oxygen reduction reaction (ORR)N, Fe-codoped carbon-based (Fe/N/C) electrocatalysts to replace currently used Pt-based catalysts has become one of the major topics in research on fuel cells. This review paper lays the emphasis on introducing the progress made over the recent five years with a detailed discussion of recent work in the area of Fe/N/C electrocatalysts for ORR and the possible Fe-based active sites. Fe-based materials prepared by simple pyrolysis of transition metal salt, carbon support, and nitrogen-rich small molecule or polymeric compound are mainly reviewed due to their low cost, high performance, long stability and because they are the most promising for replacing currently used Pt-based catalysts in the progress of fuel cell commercialization. Additionally, Fe-base catalysts with small amount of Fe or new structure of Fe/Fe<sub>3</sub>C encased in carbon layers are presented to analyze the effect of loading and existence form of Fe on the ORR catalytic activity in Fe-base catalyst. The proposed catalytically Fe-centered active sites and reaction mechanisms from various authors are also discussed in detail, which may be useful for the rational design of high-performance, inexpensive, and practical Fe-base ORR catalysts in future development of fuel cells.

**Keywords:** F/N/C electrocatalysts; oxygen reduction reaction; fuel cells; Fe-based active sites

---

## 1. Introduction

To meet the increased demand for energy in the world, one of the biggest challenges is the development of technologies that provide inexpensive, readily available, and sustainable energy. Fuel cells are among the most promising candidates for reliable and efficient conversion of alcohols into electric power in automotive and portable electronic applications on a large scale [1,2]. However, the scarcity, high cost, and poor long-term stability of Pt-Based ORR catalysts, the most widely used catalysts for the oxygen reduction reaction (ORR) in fuel cells, are main obstacles for large-scale commercialization of fuel cell technology [3,4]. Since Jasinski reported cobalt phthalocyanine as the ORR electrocatalyst in alkaline electrolytes in 1964 [5], a new era of carbon-supported non-precious metal (Co, Fe, *etc.*) and metal-free catalyst to replace the expensive Pt-based electrode in fuel cells started [6–12]. Among non-precious metal catalysts, N, Fe-codoped carbon-based (Fe/N/C) electrocatalysts (Fe-based catalysts) are the most promising candidates because some of them exhibit high ORR activity in both acidic and alkaline medium [13–15]. Fe-based catalysts can be obtained through high-temperature pyrolysis of either iron N<sub>4</sub> chelate complexes [16–21], or simple precursors of iron salts, nitrogen-containing components (aromatic [22–24] and aliphatic ligands [25–29] or other nitrogen-rich small molecules [30–36]) on carbon supports. Thus far, the state-of-the art Fe-Based catalysts exhibit much higher ORR activity and durability than those of Pt-Based catalysts in alkaline electrolytes [15,36–40] and comparable ORR activity in acidic media [7,34,41–43].

Along with the achievement of the excellent ORR activity of diverse Fe-based catalysts, the ORR mechanisms on Fe-based catalysts were also widely studied by many groups due to its importance in research and development of high-performance Fe-based ORR catalysts [21,41,44–48]. However, due to different preparation protocols used for Fe-based catalysts, there is still an ongoing debate about the active sites of these materials [45,48–50]. Therefore, there is still a long way to go in order to reach the practical usage and understanding of Fe-Based catalysts in fuel cells applications. This review addresses the current development of Fe-based ORR catalysts with a variety of different structure and properties, along with the proposed catalytically active sites and reaction mechanisms from various authors. By examining the most recent progress and research trends in both theoretical and experimental studies of Fe-based catalysts, this review provides a systematic and comprehensive discussion of the factors influencing catalyst performance as well as the future improvement strategies.

## 2. Fe-Based Catalysts

Iron, an element of the transition metal group, entered into the world of ORR catalysts in company with nitrogen in 1964 [51]. After that, Fe-based catalysts have gained increasing attention due to their promising catalytic activity for ORR, along with the utilization of abundant, low-cost precursor materials [14]. Research in Fe-based catalysts covers the non-pyrolyzed Fe-based macrocycle compounds [52–55] and pyrolyzed Fe-based macrocycle compounds [18,19,56] or some proper

Fe- and N-containing precursor materials [22,57,58]. The former are important in this field of scientific research for fundamental understanding due to their preserved well-defined structure during synthesis procedures, and the latter shows a higher ORR catalytic activity because of the introduction of high temperature heat treatment procedures (~400 to 1000 °C) to the catalyst synthesis process [13]. The structures of active sites on these Fe-based catalysts have been proposed by different groups including the structure of in-plane coordination of an iron atom and four pyridinic or pyrrolic type of nitrogen atoms embedded in a graphene-type matrix (Fe–N<sub>4</sub>/C [16,17,56,59,60] or Fe–N<sub>2+2</sub>/C [61]), the structure of coordination of an iron atom iron and two pyridinic type of nitrogen atoms embedded in a graphene-type matrix (Fe–N<sub>2</sub>/C) [60] and N-doped carbon-based structure (N–C) [62,63]. The factors of influence on ORR catalytic activity and stability of Fe-based catalysts have also been studied such as ring substituent group of non-pyrolyzed Fe-based macrocycle compounds [64,65], heat-treatment conditions [64,66,67], Fe content [68] and carbon support properties including surface nitrogen content and microporosity [31,57,69,70]. In order to produce highly active and stable Fe-based catalysts, ample approaches have been used with significant emphasis on introducing the exact effect of synthesis conditions and the nature of the catalytically active sites. Progress in this field of recent research will be divided into three sections and discussed: (1) preparation of Fe-based materials toward ORR; (2) research on structure of Fe-centered ORR active sites and ORR mechanism; and (3) stability of Fe-based ORR catalysts.

### 2.1. Preparation of Fe-Based Materials toward ORR

In 2011, Chen *et al.* [13] reviewed Fe-based catalysts in detail, so we will lay an emphasis on introducing the development of Fe-based catalysts over the most recent five years. Interestingly, it is worth pointing out that the best performing Fe-based ORR catalyst mentioned by Chen *et al.* [13] was synthesized by Dodelet *et al.* [71], which had a volumetric current density of 99 A cm<sup>-3</sup> at an *iR*-corrected voltage of 0.8 V, approaching the DOE 2010 target of 130 A cm<sup>-3</sup>. In fact, soon after that, a more exciting result was reported in August 2011 in a *Nature Communication* by the same group [72]. By using a metal-organic framework consisting of zeolitic Zn (II) imidazolate as the host for Fe and N precursors (iron (II) acetate and 1, 10-phenanthroline (Phen)), they prepared a Fe/Phen/ZIF-8 catalyst with a volumetric activity of 230 A cm<sup>-3</sup> at 0.8 V (*iR*-free) (Figure 1), a higher catalytic activity compared with that (99 A cm<sup>-3</sup>) reported in *Science* [71].

In the last five years, Fe-based materials are mainly prepared by the simple pyrolysis of transition metal salt (FeCl<sub>3</sub> [34,36,39,41,47,73–80], Fe(NO<sub>3</sub>)<sub>3</sub> [81–84], FeAc [24,74,85–88], and FeC<sub>2</sub>O<sub>4</sub> [42]), carbon support, and nitrogen-rich small molecule [34,36,78,79,85,87–89] or polymeric compound [7,39–41,90]. An important breakthrough was made by Zelenay *et al.* [7] who successfully synthesized Fe/N/C catalysts (PANI–Fe–C) via heat-treatment of polyaniline (PANI), FeCl<sub>3</sub> and carbon black (Ketjenblack EC-300J). As displayed in Figure 2a, the PANI–Fe–C catalyst shows a very high ORR onset potential (~0.93 V *vs.* RHE) in 0.5 M H<sub>2</sub>SO<sub>4</sub>, and very low H<sub>2</sub>O<sub>2</sub> yield (<1%) at all potentials. They also carried out a research into effect of heat treatment on catalytic activity of PANI-derived Fe-based catalysts in the range of 400 °C to 1000 °C (Figure 2b). The activity, as measured by the ORR onset and half-wave potential (*E*<sub>1/2</sub>) in the rotating disk electrode (RDE) polarization plots, increases to the maximum at 900 °C with a very low H<sub>2</sub>O<sub>2</sub> yield (<1%) over

the potential range from 0.1 to 0.8 V *versus* RHE, signaling virtually complete reduction of O<sub>2</sub> to H<sub>2</sub>O in a four-electron process. Although the best-performing catalyst in fuel cell testing is the more active of the two FeCo mixed-metal materials, PANI–FeCo–C, we cannot deny the fact that the ORR onset potential of PANI–Fe–C was the highest at that time [7], marking great progress in Fe-based catalysts. Before long, a new kind of Fe-based catalyst, three-dimensional (3D) N-doped graphene aerogel (N-GA)-supported Fe<sub>3</sub>O<sub>4</sub> nanoparticles (Fe<sub>3</sub>O<sub>4</sub>/N-GAs), is prepared by Wu *et al.* [86]. In studying the effects of carbon support (carbon black, graphene) on the Fe<sub>3</sub>O<sub>4</sub> nanoparticles ORR catalysts, they maintained, Fe<sub>3</sub>O<sub>4</sub>/N-GAs exhibit a more positive onset potential (–0.19 V *vs.* Ag/AgCl), higher cathodic density, lower H<sub>2</sub>O<sub>2</sub> yield, and higher electron transfer number for ORR in alkaline media than Fe<sub>3</sub>O<sub>4</sub> nanoparticles supported on N-doped carbon black (Fe<sub>3</sub>O<sub>4</sub>/N-CB) or N-doped graphene sheets (Fe<sub>3</sub>O<sub>4</sub>/N-GSSs), which further verified that choosing a proper carbon support is vital for synthesizing a high-performance ORR catalysts [86]. Recently, Sun *et al.* [34] fabricated a Fe/N/C catalysts with a ORR half-wave potential of 0.75 V (*vs.* RHE) in 0.1 M HClO<sub>4</sub> and a low H<sub>2</sub>O<sub>2</sub> yield of 2.6% at 0.4 V by pyrolyzing a composite of carbon-supported Fe-doped graphitic carbon nitride (Fe–g–C<sub>3</sub>N<sub>4</sub>@C) in the optimum conditions of Fe salt/dicyandiamide mass ratio of 1:10 and the pyrolyzed temperature at 750 °C.

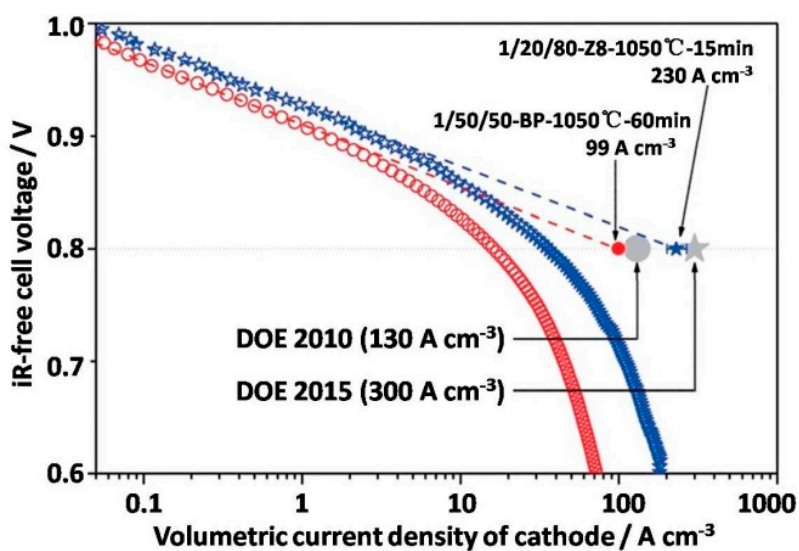


**Figure 1.** Volumetric current density of the best non-Pt catalysts in H<sub>2</sub>/air fuel cell tests at 80 °C and 100% relative humidity for cathodes [71,72] and the U.S. DOE volumetric activity target at 0.8 V (*iR*-free). Red circles: most active iron-based catalyst from previous studies, dashed red line: extrapolation of the linear range to 0.8 V, blue stars: most active iron-based catalyst from the present study, dashed blue line: extrapolation of the linear range to 0.8 V. (Reproduce with permission from Ref. [72]. Copyright © Nature Publishing Group, London, UK, 2011).

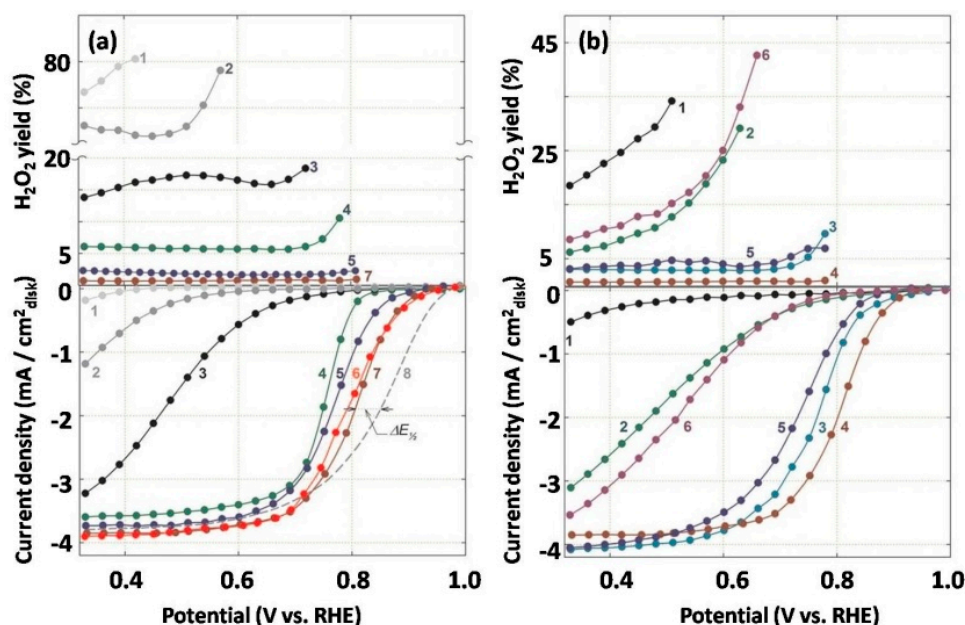


**Figure 2.** (a) Steady-state ORR polarization plots (**bottom**) and H<sub>2</sub>O<sub>2</sub> yield plots (**top**) measured with different PANI-derived catalysts and reference materials: 1, as-received carbon black (Ketjenblack EC-300J); 2, heat-treated carbon black; 3, heat-treated PANI-C; 4, PANI-Co-C; 5, PANI-FeCo-C(1); 6, PANI-FeCo-C(2); 7, PANI-Fe-C; and 8, E-TEK Pt/C (20  $\mu\text{g}_{\text{Pt}} \text{cm}^{-2}$ ). Electrolyte: O<sub>2</sub>-saturated 0.5 M H<sub>2</sub>SO<sub>4</sub> (0.1 M HClO<sub>4</sub> in experiment involving Pt catalysts (dashed line)); temperature, 25 °C. RRDE experiments were carried out at a constant ring potential of 1.2 V *versus* RHE; RDE/RRDE rotating speed, 900 rpm; and non-precious metal catalyst loading, 0.6 mg cm<sup>-2</sup>. (b) Steady-state ORR polarization plots (**bottom**) and H<sub>2</sub>O<sub>2</sub> yield plots (**top**) measured with a PANI-Fe-C catalyst in 0.5 M H<sub>2</sub>SO<sub>4</sub> electrolyte as a function of the heat treatment temperature: 1, 400 °C; 2, 600 °C; 3, 850 °C; 4, 900 °C; 5, 950 °C; and 6, 1000 °C. (Reproduce with permission from Ref. [7]. Copyright © American Association for the Advancement of Science, Washington, DC, USA, 2011).

Sun *et al.* [41] continued their work in synthesizing a Fe/N/C catalyst through high-temperature pyrolysis of the precursor containing poly-m-phenylenediamine (PmPDA) coated carbon black and FeCl<sub>3</sub> in which the Fe/N/C catalyst was denoted as PmPDA-Fe-N<sub>x</sub>/C. As depicted in Figure 3a,b, the PmPDA-Fe-N<sub>x</sub>/C catalysts pyrolyzed at 950 °C possess the highest ORR activity (11.5 A g<sup>-1</sup> at 0.80 V *vs.* RHE) and the lowest H<sub>2</sub>O<sub>2</sub> yield in 0.5 M H<sub>2</sub>SO<sub>4</sub>. They also carried out preliminary fuel cell test by employing the PmPDA-Fe-N<sub>x</sub>/C (950 °C) as cathode catalyst. The maximal power density reached 350 mW cm<sup>-2</sup> at cell voltage of 0.44 V, current density of 800 mA cm<sup>-2</sup> and the current density at 0.8 V is about 90 mA cm<sup>-2</sup> (Figure 3c,d) without back pressure applied during the fuel cell test.

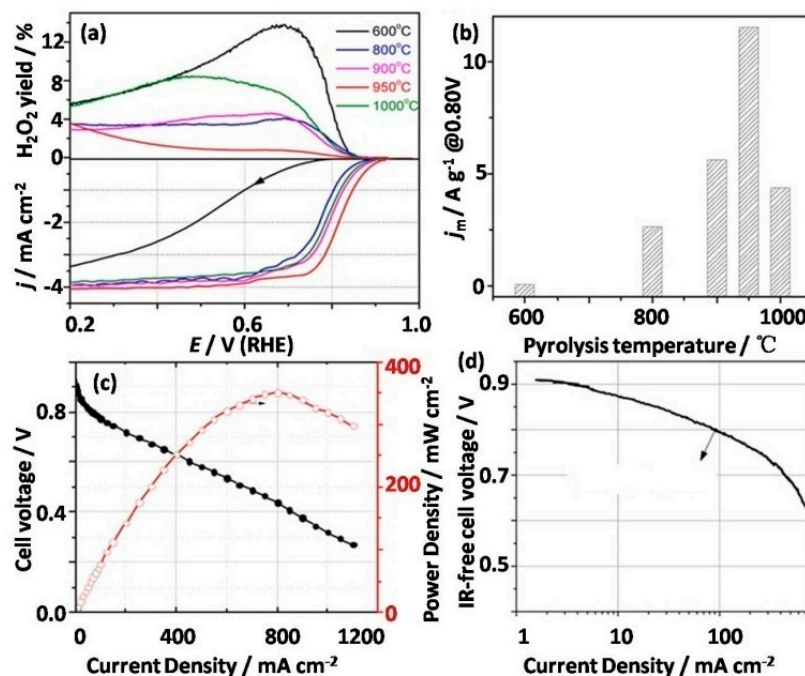


**Figure 3.** (a) ORR polarization curves and H<sub>2</sub>O<sub>2</sub> yield plots of PmPDA-Fe-N<sub>x</sub>/C catalyst prepared at different pyrolysis temperature, measured in O<sub>2</sub>-saturated 0.1 M H<sub>2</sub>SO<sub>4</sub>. Catalyst loading: 0.6 mg cm<sup>-2</sup>; Scan rate: 10 mV s<sup>-1</sup>; and Rotating speed: 900 rpm. (b) Variety of ORR mass activity at 0.80 V with pyrolysis temperature. (c) Polarization and power density plots for H<sub>2</sub>O<sub>2</sub> single fuel cell with PmPDA-Fe-N<sub>x</sub>/C as cathode catalyst at 80 °C. MEA active area: 2.0 cm<sup>2</sup>; Nafion 211 membrane; cathode catalyst loading: 4 mg cm<sup>-2</sup>; Anode catalyst: Pt/C (60 wt. %, JM) with Pt loading of 0.5 mg cm<sup>-2</sup>. No back pressure was applied. (d) Plot of  $iR$ -free cell voltage *versus* the logarithm of current density. (Reproduce with permission from Ref. [41]. Copyright © American Chemical Society, Washington, DC, USA, 2014).

Compared to pyrolysis of simple Fe salt, the Fe-based catalysts prepared via heat-treatment iron phthalocyanines (Pc)/porphyrins and their derivatives supported on carbon materials or some synthesized Fe-based macrocycle compounds have also attracted widely public attention in recent years [15,38,47,55,77,91,92]. Among all the FePc-based catalysts (FePc/SWCNT, FePc/DWCNT, and FePc/MWCNT), synthesized by Morozan *et al.* [55], dispersing iron(II) phthalocyanine on different types of carbon nanotubes (SWCNTs, DWCNTs, MWCNTs), FePc/MWCNT catalysts exhibit the best ORR performance in alkaline electrolyte close to the Pt/C reference. In 2012, by reacting the pyridine-functionalized graphene with iron-porphyrin, a graphene-metalloporphyrin metal organic framework (MOF) with enhanced catalytic activity for ORR was synthesized by Jahan *et al.* [77]. The authors claimed that the addition of pyridine-functionalized graphene changes the crystallization process of iron-porphyrin in the MOF, increase its porosity, and enhances the electrochemical charge transfer rate of iron-porphyrin, and therefore, enhance the ORR catalytic activity of these Fe-based catalysts [77]. After that, an exciting result was reported in *Nature Communication* by the Cho group [91]. A composite of FePc and SWCNTs (FePc-Py-CNTs) from covalent functionalization of SWCNTs, taking advantage of the diazonium reaction, was synthesized by anchoring pyridyl (Py)

groups on the walls of CNTs, prior to FePc coordinated to Py–CNTs through the bond formed between nitrogen atom in pyridine and iron center in FePc (Figure 4a) [91]. The as-synthesized composites show a higher ORR catalytic activity with a half-wave potential ( $E_{1/2}$ ) at 0.915 V (vs. RHE) than that of the state-of-the-art Pt/C with  $E_{1/2}$  value at 0.88 V (Figure 4b). Theoretical calculations made by the authors suggest that the rehybridization of Fe 3d orbitals with the ligand orbitals coordinated from the axial direction results in a significant change in electronic and geometric structure, which greatly increases the ORR catalytic activity of catalysts [91]. Differ from the CNTs used as carbon support of FePc by Cho *et al.*, using chemically reduced graphene as the carbon support of FePc, Chen *et al.* [38] successfully synthesized a g-FePc catalyst through forceful  $\pi$ – $\pi$  interaction. The results of electrochemical measurements suggest that g-FePc catalyst possesses prominent ORR catalytic activity, which is comparable with commercial Pt/C in both onset potential and current density in 0.1 M KOH [38]. Furthermore, Liu's group [92,93] and Dai's group [15] also devote themselves to synthesize highly active Fe-based catalysts started from preparation of N-containing Fe-porphyrin complex or the solid-state synthesis of zeoliticimidazolate frameworks. Although the Fe-based catalysts prepared via heat-treatment iron phthalocyanines (Pc)/porphyrins and their derivatives supported on carbon materials or some synthesized Fe-based macrocycle compounds seems to be a little complicated or high-cost relative to pyrolysis of transition metal salt carbon support, and nitrogen-rich small molecule, still plays an important role in the preparation of ORR catalysts and research of ORR active sites.

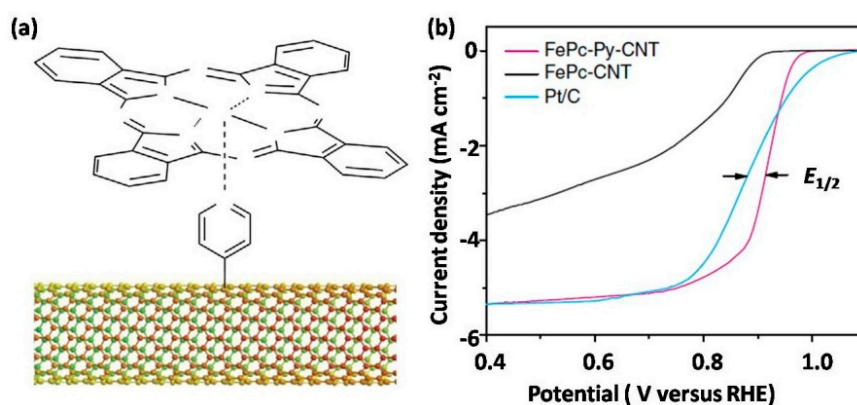


**Figure 4.** (a) Schematic diagram of the structure of FePc–Py–CNTs composite; and (b) linear scanning voltammograms of FePc–CNTs, FePc–Py–CNTs and commercial Pt/C catalyst. (Reproduce with permission from Ref. [91]. Copyright © Nature Publishing Group, London, UK, 2013).

It is not a unique instance, a new kind of highly active material, N-doped Fe or Fe<sub>3</sub>C encapsulated in carbon support (CNTs or Graphitic layers), has been reported by many groups [39,67,87,94–97]. In 2012, Chen *et al.* [94] reported a synthetic strategy that enables synthesis of nitrogen-enriched core-shell structured catalysts with iron-based composite (Fe/Fe<sub>3</sub>C) nanorods as the core and graphite carbon as the shell (N–Fe/Fe<sub>3</sub>C@C) (Figure 5a). The N–Fe/Fe<sub>3</sub>C@C shows significantly improved activities and advanced kinetics for ORR in neutral phosphate buffer solution (PBS) compared with the commercial Pt/C catalysts (Pt 10%). The authors proposed that the doped N and core-Fe<sub>3</sub>C in the N–Fe/Fe<sub>3</sub>C@C play key roles in improving the catalytic performance for ORR [94]. Soon after that,

Lee *et al.* [94] found that the Fe/Fe<sub>3</sub>C-functionalized melamine foam exhibited good ORR activities in alkaline media. Referring to the possibly important role of the Fe<sub>3</sub>C phase in the ORR, Hu *et al.* [94] synthesized a Fe-based catalyst in the form of hollow spheres comprising uniform Fe<sub>3</sub>C nanoparticles encased by a graphitic layer (Fe<sub>3</sub>C/C) (Figure 5b) via high-pressure pyrolysis. The results of rotating disk electrode and rotating ring disk electrode measurement suggested that Fe<sub>3</sub>C/C catalyst exhibited a high ORR activity and stability in both acidic and alkaline media partly due to the activation of the surrounding graphitic layers by the encased carbide nanoparticles, and making the outer surface of carbon layer active towards the ORR [97]. Recently, Xing *et al.* [39] synthesized a Fe-based catalyst with iron carbide encapsulated in N-doped graphitic layers (Fe<sub>3</sub>C/NG) (Figure 5c), which also possesses high ORR activity and stability and further affirmed the importance of the structure of Fe/Fe<sub>3</sub>C encased in carbon layers. In fact, Fe encapsulated within carbon nanotubes (Figure 5d,e) as ORR catalysts has also been reported by both the Zelenay group [87] and the Bao group [95]. So we can excitedly find a fact that Fe element will play an important role in the ORR wherever it locates on the surface of N-doped carbon materials bonded with N or is encased by carbon layers.

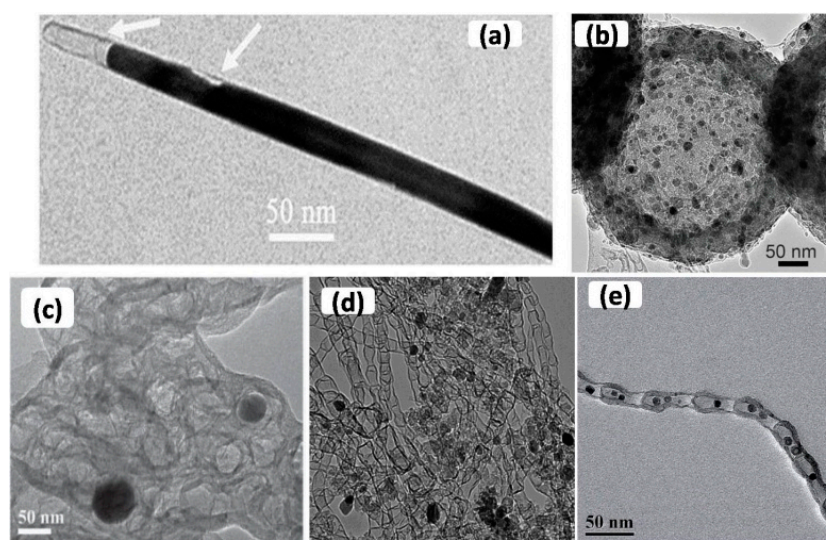


**Figure 5.** (a) TEM image of simple N-Fe/Fe<sub>3</sub>C/C nanrod with close-end graphite shell (Reproduce with permission from Ref. [94]. Copyright © WileyY-VCH Verlag GmbH & Co. KGaA, Weinheim, Germany, 2012). (b) TEM image of one typical hollow catalyst sphere of Fe<sub>3</sub>C/C (Reproduce with permission from Ref. [97]. Copyright © WileyY-VCH Verlag GmbH & Co. KGaA, Weinheim, Germany, 2014). (c) TEM image of Fe<sub>3</sub>C/NG; (Reproduce with permission from Ref. [39]. Copyright © WileyY-VCH Verlag GmbH & Co. KGaA, Weinheim, Germany, 2015). (d) TEM of the N-Fe-CNT/CNP composite (Reproduce with permission from Ref. [87]. Copyright © Nature Publishing Group, 2013). (e) TEM of image of Pod-Fe (Reproduce with permission from Ref. [95]. Copyright © WileyY-VCH Verlag GmbH & Co. KGaA, Weinheim, Germany, 2013).

It is recognized widely that Fe-doping would enhance the performance of N-doped catalyst. Among the transition metals (Mn, Fe, Co, Ni, and Cu), Fe, N-codoped catalysts exhibits the highest ORR

activity [98], which fully displays the importance of Fe-based catalysts for ORR. Interestingly, Dai *et al.* [43] synthesized nanotubes-graphene (NT-G) complexed, few-walled carbon nanotubes with the outer wall partially unzipped by harsh oxidation in  $\text{KMnO}_4/\text{H}_2\text{SO}_4$ , which exhibit a high activity, excellent tolerance to methanol and superior stability in both acidic and alkaline solutions. The authors claimed that the NT-G contains small amount of irons (1.10 wt. %) originated from nanotube growth seeds, and nitrogen impurities, which facilitate the formation of catalytic sites and boost the activity of the catalyst, and the role of iron in forming active ORR catalytic sites in the NT-G complex is proved by  $\text{CN}^-$  Poisoning experiments [43]. The role of extremely small amount of iron in ORR was further verified by Xu's group [36]. The authors synthesized a series of Fe-based catalysts by tuning the Fe content and codoping with nitrogen on cheap carbon black (CB) over a wide range from 0.02 to 20 wt. % (Figure 6a) and found that the optimal catalyst with a trace Fe content (0.05 wt. %) showed a superior high performance compared with commercial Pt/C in 0.1 M KOH (Figure 6b). Then after Xu, Pumera's group [99] demonstrated that residual manganese-based metallic impurities in graphene also play an extremely active role in the electrocatalysts of ORR on supposedly metal-free graphene electrode, which indirectly affirmed the role of a small amount of iron in other carbon-based ORR catalysts. Recently, Chen *et al.* [40] fabricated a series of self-supported N-doped mesoporous carbons with a trace amount of Fe (Fe-N/C). Electrochemical measurements revealed that Fe-N/C with an iron content of 0.24 at. % prepared at 800 °C was the best catalysts (Fe-N/C-800), with a more positive onset potential (0.98 V vs. RHE), higher diffusion-limited current, higher selectivity, higher stability, and stronger tolerance against methanol crossover than commercial Pt/C catalysts in 0.1 M KOH [38]. Interestingly, the results of cyanide poisoning and hot  $\text{H}_2\text{SO}_4$  leaching for Fe-N/C-800 suggested that ORR was primarily due to iron-free active sites that arose most likely from nitrogen doping and the contributions of Fe-base active sites was small [40]. From all of the above, we can suggest that whether the small amount of iron will form active ORR catalytic sites or not is greatly dependent on the conditions for the preparation of Fe-based catalyst.

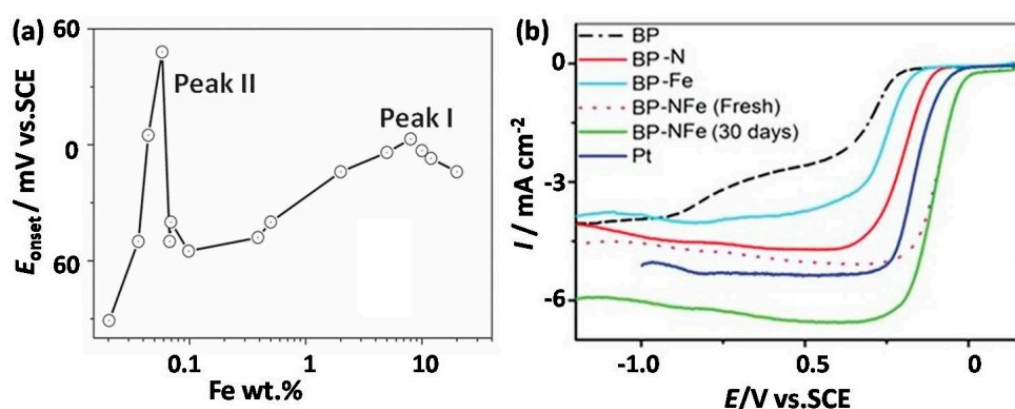


**Figure 6.** (a) Fe-content dependence of Fe-based catalysts. (b) RDE polarization curves of pure BP, BP-N, BP-Fe, BP-NFe, and Pt/C in  $\text{O}_2$ -saturated 0.1 M KOH with a scan rate of  $5 \text{ mV s}^{-1}$  and rotation speed of 1600 rpm. (Reproduce with permission from Ref. [36]. Copyright © WileyY-VCH Verlag GmbH & Co. KGaA, Weinheim, Germany, 2013).

**Table 1.** Electrocatalytic performance (onset potential ( $E_o/V$  vs. RHE) and half-wave potential ( $E_{1/2}/V$  vs. RHE)) of recently reported Fe-based catalysts for ORR and the corresponding test results ( $T/^\circ\text{C}$ , test temperature; OCV/V, open-circuit voltage; MPD/ $\text{mW cm}^{-2}$ , and maximum power density) of fuel cell ( $\text{H}_2\text{-O}_2$  fuel cell, acid/alkaline direct methanol fuel cell (DMFC) or Zn-air fuel cell).

Catalysts	Acid or Alkaline	$E_o$ (V vs. RHE)	$E_{1/2}$ (V vs. RHE)	Cell tests, $T(^\circ\text{C})$ , OCV (V) and MPD ( $\text{mW cm}^{-2}$ )	Reference (Year)
PANI-Fe-C	0.1 M $\text{HClO}_4$	$\sim 0.93$	/	$\text{H}_2\text{-O}_2$ , 80, $\sim 0.9$ , $< 550$	Ref. [7] (2011)
C-COP-P-Fe	0.1 M KOH	ca. 0.98	/	/	Ref. [15] (2014)
	0.1 M $\text{HClO}_4$	ca. 0.89	/	/	
BP-NFe	0.1 M KOH	0.045 vs. SCE	$-0.089$ vs. SCE	DMFC, 60, 0.8, 16.6	Ref. [36] (2013)
	0.5 M $\text{H}_2\text{SO}_4$	0.6 vs. SCE	/	/	
g-FePc	0.1 M KOH	0.98	0.88	/	Ref. [38] (2013)
$\text{F}_3\text{C}/\text{NG-800}$	0.1 M KOH	1.03	0.86	DMFC, 60, 0.75, 31	Ref. [39] (2015)
	0.1 M $\text{HClO}_4$	0.92	0.77	DMFC, 60, 0.87, 19	
Fe-N/C-800	0.1 M KOH	0.98	/	/	Ref. [40] (2015)
	0.1 M $\text{HClO}_4$	0.77	/	/	
PmpDA-Fe-N <sub>x</sub> /C	0.1 M $\text{H}_2\text{SO}_4$	$\sim 0.93$	/	$\text{H}_2\text{-O}_2$ , 80, $\sim 0.9$ , 350	Ref. [41] (2014)
NT-G	0.1 M KOH	$> 1.05$	0.87	/	Ref. [43] (2012)
	0.1 M $\text{HClO}_4$	$\sim 0.89$	0.76	/	
$\text{Fe}_3\text{O}_4/\text{N-GAs}$	0.1 M KOH	$-0.19$ vs. Ag/AgCl	/	/	Ref. [86] (2012)
N-Fe-CNT/CNP	0.1 M NaOH	$> 1.05$	0.93	/	Ref. [87] (2013)
FePc-Py-CNTs	0.1 M KOH	$> 1.05$	0.915	/	Ref. [91] (2013)
$\text{Zn}(\text{mlm})_2\text{TPIP}$	0.1 M $\text{HClO}_4$	0.902	0.76	$\text{H}_2\text{-O}_2$ , 80, $\sim 0.95$ , 620	Ref. [92] (2014)
PFeTTPP-1000	0.1 M $\text{HClO}_4$	0.93	0.76	$\text{H}_2\text{-O}_2$ , 80, 0.9, 730	Ref. [93] (2013)
N-Fe/ $\text{Fe}_3\text{C}@C$	0.1 M PBS	0.21 vs. Ag/AgCl	/	/	Ref. [94] (2012)
Pod-Fe	0.1 M $\text{H}_2\text{SO}_4$	0.5 vs. Ag/AgCl	0.3 vs. Ag/AgCl	$\text{H}_2\text{-O}_2$ , 70, 0.7, /	Ref. [95] (2013)
Ar-800	0.1 M KOH	$\sim 0.05$ vs. Hg/HgO	/	Zn-air, 1.2, 200	Ref. [96] (2013)
$\text{Fe}_3\text{C}/C-800$	0.1 M KOH	1.05	0.83	/	Ref. [97] (2014)
	0.1 M $\text{HClO}_4$	ca. 0.90	ca. 0.73	/	

Table 1 shows the representational results of electrocatalytic ORR performance and fuel cell tests of recently reported Fe-based catalysts in both acid medium and alkaline medium. Although the ORR performance of Fe-based catalysts in alkaline medium has outperformed that of commercial Pt/C, its ORR performance in acid media is still inferior to that commercial Pt/C. The ORR onset potential of Fe-based catalysts in alkaline has reached the value of 1.05 V (*vs.* RHE) [43,87,91], while the highest value of ORR onset potential to date in acid medium is just close to 0.93 V (*vs.* RHE) [7,39,41,93]. The reason why the Fe-based catalysts own the lower ORR catalytic activity in acid than that of in alkaline medium will be discussed in Section 2.2. In addition, considering the practicality of Fe-based catalysts for ORR in fuel cell, the best performing Fe-based ORR catalysts in acid condition reported to date is synthesized by Liu's group [92,93], who made H<sub>2</sub>-O<sub>2</sub> fuel cell tests by using the as-prepared Fe-based materials as cathode catalysts and commercial Pt/C as anode catalysts and get a highly maximum power density of fuel cell tests of 730 mW cm<sup>-2</sup> [93] and 620 mW cm<sup>-2</sup> [92] in 2013 and 2014, respectively. However, regarding the ORR activity of Fe-based catalysts in acid, the actual volumetric activity of even the most active Fe-based catalysts needs to be improved. Regarding the ORR stability of Fe-based catalysts in both alkaline media and acid media, the stability tests are generally run at low current density or low power level, which are not real conditions for fuel cell operation. Hence, there is still a long way to go in order to reach the practical usage and understanding of Fe-based catalysts in fuel cells for commercial applications.

In summary, Fe-based catalysts represent a promising family of non-precious metal ORR catalyst candidates. It is obvious that the preparation conditions of Fe-based catalyst have a direct influence on the resulting Fe-based ORR electrocatalyst materials. A proper N-doped carbon support or N-enriched precursor selected for Fe-based catalyst is also vital for the final ORR catalytic activity. Of course, Fe is thus an already profoundly studied dopant for N-doped ORR electrocatalysts and will play a significant role in the further ongoing process within this field.

## 2.2. Research on Structure of Fe-Centered ORR Active Sites and ORR Mechanism

Considering the most recent progress of Fe-based catalysts, insight into formation mechanisms and structures of ORR active sites is also an ongoing task in the research and development of Fe-based catalysts for fuel cell applications. The current proposed active sites, containing edge plane FeN<sub>2</sub>/C and FeN<sub>4</sub>/C [60] species as well as basal plane macrocyclic FeN<sub>4</sub>/C [19,20] species, are mainly speculated by data obtained from X-ray photoelectron spectroscopy (XPS) [19,100], time-of-flight secondary ion mass spectroscopy (TOF-SIMS) [45,60], X-ray absorption fine structure [18,60], and Mossbauer spectroscopy [17,19]. In 2008, Dodelet's group [61] claimed that the majority of active sites consist of a Fe-N<sub>4</sub>/C (labeled by the authors as FeN<sub>2+2</sub>/C) configuration bridging two adjacent graphene crystallites. Recently, Dodelet *et al.* [73] continue their work to clarify the origin of the enhanced PEM fuel cell performance of catalysts prepared by the procedures described in *Science* [71] and *Nature Communication* [72]. Among all the Fe-N<sub>4</sub>-like species they reported, ORR activity is only attributed to Fe-N<sub>4</sub>/C and N-Fe-N<sub>2+2</sub>/C, which are the structure of coordination of nitrogen atoms and the iron atoms of Fe-N<sub>4</sub>/C [73]. The former is a well-known site typically found in heat-treated carbon supported or unsupported porphyrins, and the latter is a very new kind of active composite N-Fe-N<sub>2+2</sub>-NH<sup>+</sup> site, which is the high activity state of N-Fe-N<sub>2+2</sub>/C. More importantly,

Fe–N<sub>4</sub>/C and N–Fe–N<sub>2+2</sub>/C are more available in catalysts pyrolyzed in Ar + NH<sub>3</sub> atmosphere than in only Ar or NH<sub>3</sub> [73]. After the Dodelet's report in 2008 [61], Kramm *et al.* [59] firstly attributed improved ORR kinetics of these Fe–N<sub>4</sub> centers to Fe ion centers with higher electron densities. The authors made a further study on the structure of catalytic site in Fe-based catalysts for ORR via analyzing the Fe-species existed in the Fe-based catalysts prepared by impregnation of iron acetate on carbon black followed by heat-treatment in NH<sub>3</sub> at 950 °C [44]. Five different Fe-species were detected in the Fe-based catalysts containing 0.03 to 1.55 wt. % Fe: three doublets assigned to molecular FeN<sub>4</sub>-like sites with their ferrous ions in a low (D1), intermediate (D2) or high (D3) spin state (Figure 7), and two other doublets assigned to a single Fe-species (D4 and D5) consisting of surface oxidized nitride nanoparticles [44]. Among the five Fe-species identified by <sup>57</sup>Fe Mossbauer spectroscopy in these catalysts, the authors maintained, only D1 and D3 display catalytic activity for the ORR in acid medium, with D3 featuring a composite structure with a protonated neighbor basic nitrogen and being far from the most active species [44]. These findings reveal that when focusing on the development of Fe-based catalysts with improved active site densities, it is possible to tune the electronic and structure properties of these active site structures, or develop Fe-based catalysts with higher ORR-activity by developing ways to make a larger fraction of the available Fe-atoms form more of the most ORR-active composite N–FeN<sub>2+2</sub>...N<sub>prot</sub>/C (D3) sites.

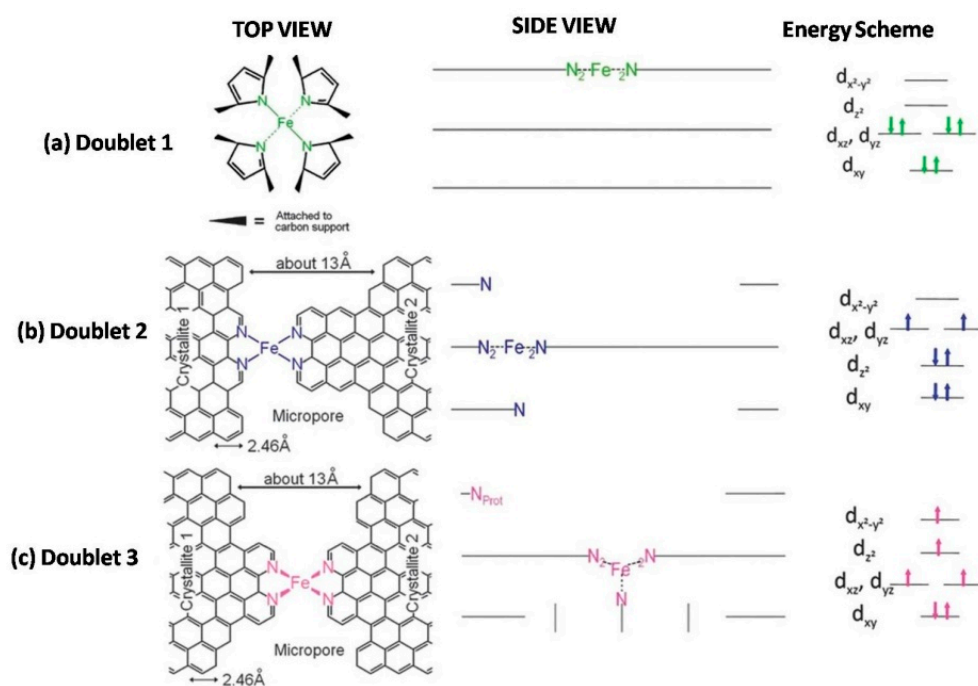
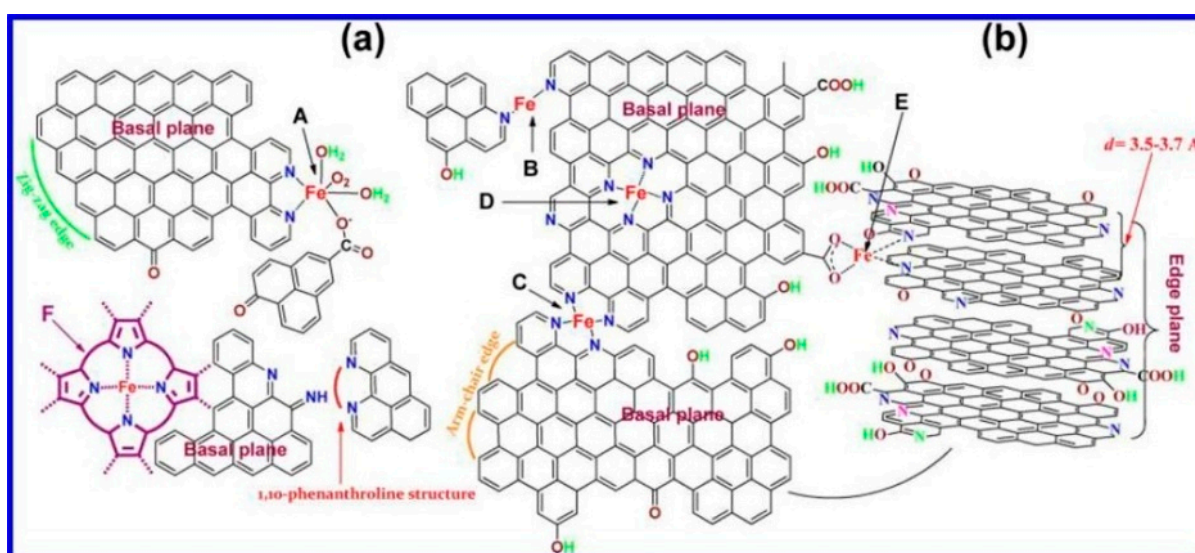


**Figure 7.** Side views and top views of the proposed structures of: (a) the FeN<sub>4</sub>/C catalytic site in heat-treated, macrocycle-based catalysts assigned to Mossbauer doublet D1; (b) the FeN<sub>2+2</sub>-like micropore-hosted site found in the catalyst prepared with iron acetate and heat-treated in ammonia assigned to doublet D2; and (c) the N–FeN<sub>2+2</sub>-like composite site, where N–FeN<sub>2+2</sub> is assigned to doublet D3. In all side views, graphene planes are drawn as lines. (Reproduce with permission from Ref. [44]. Copyright © Royal Society of Chemistry, London, UK, 2012).

Recently, Chen *et al.* [45] proposed two possible formation mechanisms for the catalytically active sites occurring during high-temperature pyrolysis treatments through  $\text{CN}^-$  ions poisoning experiments, dependent on the specific type of precursor and synthesis methods utilized. The proposed structures of high-temperature-treated Fe-based catalysts are depicted in Scheme 1. These active sites include 1,10-phenanthroline (phen)-like iron complexes (A and C) [35,60], single pyridine-like iron complexes (B and E), and macrocyclic-like iron complexes (D and F) [20,45]. The authors claimed that utilizing aromatic iron complex ligands in inert atmospheres, catalytically active sites (C and D) will be formed in the layers of material deposition and will build up on the surface of the carbon support, which will decrease the porosity of surface layer and results in the majority of active sites being inaccessible, entrapped in the subsurface layers, and such that leading to inhibited reactant and product mass transfer to and from the catalytically active sites. On the contrary, Fe-based catalysts prepared by pyrolyzing nonaromatic ligands, such as  $\text{NH}_3$ , and aliphatic diamines can result in the simultaneous production of the second active sites (A, B, and E) and well-connected channels [45]. The research provides valuable insight toward the development of Fe-based catalysts with improved ORR activity and stability. In 2013, Kattale *et al.* [50] performed first-principles density functional theory (DFT) calculations to investigate the reaction pathway of ORR on Fe-N<sub>4</sub> catalytic clusters formed between pores in graphene supports. The DFT results indicate that formation of Fe-N<sub>4</sub> clusters at the edges of graphitic pores is energetically feasible and ORR would proceed on the assuming a pathway that follows the chemical reactions: (1)  $\text{O}_2 \rightarrow * \text{O}_2$  (adsorption); (2)  $* \text{O}_2 + (\text{H}^+ + \text{e}^-) \rightarrow * \text{OOH}$ ; (3)  $* \text{OOH} + (\text{H}^+ + \text{e}^-) \rightarrow 2 * \text{OH}$ ; and (4)  $2 * \text{OH} + 2(\text{H}^+ + \text{e}^-) \rightarrow 2 \text{H}_2\text{O}$ . The authors predicted that Fe-N<sub>4</sub> clusters near graphitic pores could promote the  $4\text{e}^-$  ORR with a single active site contain central Fe atom and four surrounding N atoms due to the split of O–O bond in the reactant  $\text{O}_2$  during the interaction of intermediate HOOH with the Fe-N<sub>4</sub> clusters in the above ORR pathway [50]. The theoretical study provides an explanation to the experimentally observed  $4\text{e}^-$  ORR on heat treated Fe/N/C electrocatalysts and certified the Fe-centered active sites of these Fe/N/C electrocatalysts. More recently, the highly Fe-centered active sites was also verified by Ozkan's group [46] via  $\text{H}_2\text{S}$  poisoning experiments, which suggested that Fe plays a critical role in catalyzing ORR for Fe/N/C catalysts. Interestingly, except the above experimental work mentioned in Section 2.1, in combination with the XRD and XPS results of the pyrolyzed Fe/N/C catalysts, Sun *et al.* [34] propose that the ORR active sites are closely related to  $\text{Fe}_3\text{N}$  and both pyridinic N (which may bond to  $\text{Fe}^{\text{III}}$  to form  $\text{Fe}_3\text{N}$ ) and quaternary N in the pyrolyzed Fe/N/C composites are conducive to catalyze the ORR and can serve as catalytically active sites for oxygen reduction in acid media. Through systematic of the effects of a series of inorganic molecules and ions ( $\text{Cl}^-$ ,  $\text{F}^-$ ,  $\text{Br}^-$ ,  $\text{SCN}^-$ ,  $\text{SO}_2$  and  $\text{H}_2\text{S}$ ) on the ORR activity, they further maintained, the active site of the Fe/N/C in acidic solutions contain Fe element and its valence state is mainly  $\text{Fe}^{\text{III}}$  since this catalyst is not sensitive to CO and  $\text{NO}_x$  but distinctly sensitive to  $\text{F}^-$  ion. The new insight into the active site nature of the Fe/N/C through molecule/ion probe is of very useful in rational design of high performance Fe-based catalysts for ORR in acid media [41].

Additionally, the ORR catalytic activity of Fe-based catalysts prepared by Mukerjee *et al.* [101] in 2011 through a pyrolysis in  $\text{NH}_3$  is mostly imparted by acid-resistant Fe-N<sub>4</sub> sites whose turnover frequency for  $\text{O}_2$  reduction can be regulated by fine chemical changes of the catalyst surface. The authors claimed that surface N-groups could be protonated at pH 1 and subsequently bind anions, resulting in decreased activity for the  $\text{O}_2$  reduction, and the anions can be removed chemically or

thermally to restore the activity of acid-resistant Fe–N<sub>4</sub> sites [101]. The implications of the findings reported in this work suggested that optimizing the catalyst/electrolyte interface to prevent anion binding is required to combine high activity and durability of Fe-based catalysts. In fact, Mayer *et al.* [21,102,103] has also investigated the selectivity for four-electron reduction to H<sub>2</sub>O or two-electron reduction to H<sub>2</sub>O<sub>2</sub> of Fe-based catalysts in iron-porphyrin complexes. Using Iron<sup>(III)</sup> meso-tera(2-carboxyphenyl)-porphine chloride and its isomer as ORR electrocatalysts, the authors found that the Fe-based catalysts containing proton relays closed to the redox center in the second coordination sphere of iron-porphyrin complexes have a high selectivity for four-electron reduction to H<sub>2</sub>O, which suggested the importance of catalyst design for selectivity in Fe-based catalysts [102]. Recently, however, the authors verified that the nature of the catalyst film on a carbon electrode has an effect as large as changing the structure of the molecular catalyst itself [21].



**Scheme 1.** Possible Iron Active Site Structures on Nanocrystal Graphite: (a) top and (b) side view (Reproduce with permission from Ref. [45]. Copyright © American Chemical Society, Washington, DC, USA, 2012).

Mukerjee *et al.* [104] continued their research on ORR mechanism of pyrolyzed Fe-based catalysts in alkaline medium and identified an activity descriptor based on principles of surface science and coordination chemistry. Using iron(III) meso-tetraphenylporphine chloride (FeTPPCl) as a model system, the authors elucidate inner- vs. outer-sphere ORR mechanisms and active-site structure evolution on pyrolyzed Fe-based catalysts. As depicted in Figure 8a, in alkaline media, taking platinum surface as a starting point of illustration, the well-known electrocatalytic inner-sphere electron transfer (ISET) mechanism (Figure 8a, inset i) involves chemisorptions of desolvated O<sub>2</sub> on an oxide-free Pt-site (Figure 8a, when M is represented as Pt) leading to a direct/series 4e<sup>−</sup> ORR pathway without desorption of reaction intermediates and the coexistence of an outer-sphere electron transfer (OSET) mechanism (Figure 8a, inset ii), wherein the noncovalent hydrogen bonding forces between specifically adsorbed hydroxyl species (OH<sub>ads</sub> acting as an outer-sphere bridge) and solvated O<sub>2</sub> (localized in outer-Helmholtz plane) promote a 2e<sup>−</sup> reduction pathway forming HO<sub>2</sub><sup>−</sup> anion [104]. Therefore, the goal of promotion of an electrocatalytic inner-sphere reaction mechanism for a complete 4e<sup>−</sup> ORR

process in alkaline electrolytes can be achieved via facilitation of direct adsorption of desolvated O<sub>2</sub> on OH<sub>ads</sub>-free active sites and avoiding the precipitous outer-sphere reaction of solvated O<sub>2</sub> with OH<sub>ads</sub> covered active sites [104]. In the system of Fe–N<sub>4</sub>/C active sites, the 4e<sup>−</sup> electrocatalytic inner-sphere electron transfer mechanism in dilute alkaline media is shown in Figure 8b, wherein O<sub>2</sub> displaces the OH<sup>−</sup> species and chemisorbs directly on the Fe<sup>2+</sup> active site [104]. The lability of the axial OH<sup>−</sup> anion is due to the redox mechanism of ORR that ensures the reduction of pentacoordinated (H)O–Fe<sup>3+</sup>–N<sub>4</sub> to the square-planar Fe<sup>2+</sup>–N<sub>4</sub> active site where axial ligation is available for direct O<sub>2</sub> chemisorption. This ensures that the precipitous OSET mechanism is avoided on Fe–N<sub>4</sub>/C active sites leading to direct chemisorption of O<sub>2</sub> on the metal center via an inner-sphere mechanism. Once molecular O<sub>2</sub> adsorbs on the Fe<sup>2+</sup> active site, via the superoxo and the ferric-hydroperoxyl states, the reaction proceeds to the ferrous-hydroperoxyl adduct, which is very critical since its stability determines the product distribution and ORR electrocatalytic activity. For pH > 12, the Lewis basic nature of the anionic hydrogen peroxide intermediate (HO<sub>2</sub><sup>−</sup>, pK<sub>a</sub> ≈ 11.6) leads to its apparent stabilization on Lewis acidic Fe<sup>2+</sup> active sites via the formation of stabilized Lewis acid-base adduct, which ensures that the catalytic cycle in alkaline media undergoes complete 4e<sup>−</sup> transfer (Figure 8b) to regenerate the active site via the formation of ferric-hydroxyl species. However, in acidic media the analogous ferrous-hydroperoxyl adduct is Fe<sup>II</sup>–(OHOH), wherein the protonated nature of the hydrogen peroxide intermediate (H<sub>2</sub>O<sub>2</sub>) negates its Lewis basic character and leads to its apparent destabilization on Fe<sup>2+</sup>–N<sub>4</sub>/C active site, which hence leads to higher overpotential for ORR in acidic media necessitating secondary sites to further reduce or disproportionate H<sub>2</sub>O<sub>2</sub>. Therefore, the author claimed that Fe–N<sub>4</sub>/C active sites are more active for ORR in alkaline media than that of in acid media [104]. In addition, Fe–N<sub>4</sub>/C active sites, the authors maintained, which was covalently integrated into the π-conjugated carbon basal plane during the pyrolysis step, could cause a dramatic anodic shift of ~600–900 mV in the metal ion's redox potential. Since the carbon basal plane constitutes an integral part of the active site due to the electron-donating/withdrawing capability of carbon support, the authors further claimed that tuning electron donating/withdrawing capability of the carbon basal plane, conferred upon it by the delocalized π-electrons, (i) causes a downshift of e<sub>g</sub>-orbitals (d<sub>z</sub><sup>2</sup>), thereby anodically shifting the metal ion's redox potential, and (ii) optimizes the bond strength between the metal ion and adsorbed reaction intermediates thereby maximizing oxygen-reduction activity [104]. The report makes it being possible to tune the catalytic activity of the class of pyrolyzed Fe-based catalysts by experimentally controlling the degree of π-electron delocalization of the carbonaceous surface and open the door to the development of more active and stable electrocatalysts based on Fe-centered active sites on novel π surfaces. Recently, Mukerjee *et al.* [48] made a further study on the various structural and functional forms of the active centers in pyrolyzed Fe-based catalysts in both ranges of pH and confirmed the single site 2e<sup>−</sup> × 2e<sup>−</sup> mechanism in alkaline media on the primary Fe<sup>2+</sup>–N<sub>4</sub> centers and the dual-site 2e<sup>−</sup> × 2e<sup>−</sup> mechanism in acid media with the significant role of the surface bound coexisting Fe/Fe<sub>x</sub>O<sub>y</sub> nanoparticles (NPs) as the secondary active sites by employing a combination of *in situ* X-ray spectroscopy and electrochemical methods. From what has been discussed above, we can draw the conclusion that Fe<sup>3+</sup> is mainly the active sites for ORR in acid media [34,41], while Fe<sup>3+</sup> and Fe<sup>2+</sup> are both play vital role for ORR in alkaline [48,104]. On the contrary, surface N-groups protonation is not beneficial for ORR activity [101,102].

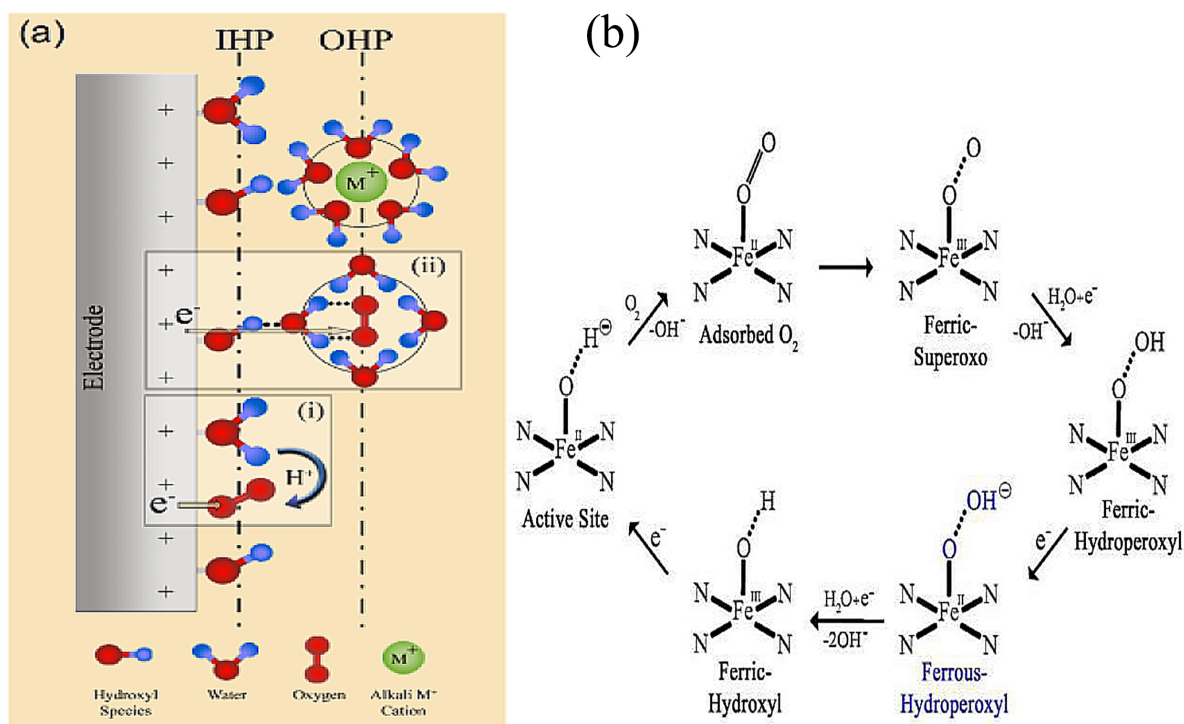


**Figure 8.** Proposed ORR mechanism. (a) Schematic illustration of inner-sphere (inset i) and outer-sphere (inset ii) electron transfer mechanisms during ORR in alkaline media. (b) Catalyst cycle showing the redox mechanism involved in ORR on pyrolyzed Fe-N<sub>4</sub>/C active sites in dilute alkaline medium; (IHP, inner Helmholtz plane; OHP, outer Helmholtz plane) (Reproduce with permission from Ref. [104]. Copyright © American Chemical Society, 2013).

### 2.3. Stability of Fe-Based ORR Catalysts

Although Fe-based catalysts with Fe-N<sub>4</sub> sites initially exhibit a highly catalytic activity in acidic medium, their durability is still insufficient [105]. Therefore, bridging the gap between the attributes responsible for high activity and high durability has become the main challenge facing Fe-based catalysts. In recent years, the stability of Fe-based ORR catalysts in alkaline medium has shown to be better than that of in acid medium [105]. Xu's group [36] has found the ORR performance in alkaline medium of their Fe-based catalysts containing extremely small amount of iron tend to be improved with larger diffusion-limiting current when the catalysts ink was re-tested after 30 days. The authors attributed the increase of diffusion-limiting current to the increase of oxygen diffusion coefficient in the microenvironment of the catalyst layer or the exposure of more active sites [36]. Compared to the higher stability in alkaline media, the reason for the degradation of Fe-based catalysts in the acidic environment during the ORR process has been attributed to the corrosion/oxidation of the active center and carbon support, attack by hydrogen peroxide of both the Fe and N sites, and the oxidation of the pyridinic active sites [106]. In fact, before the results reported by Xu's group [36], Zelenay's group [7,87] had already reported a phenomenon about the Fe-based catalysts durability, in which the authors make a cycling durability test in O<sub>2</sub>-saturated solution in 0.1 M NaOH for their Fe-based ORR catalysts and found that the ORR performance of these catalysts not only did not become poor

but shows a positive shift in the  $E_{1/2}$  value [87], which is similar to their previous report about the potential shift with cycling observed with non-precious metal ORR catalysts at high current densities in acid medium in proton conducting fuel cells [7]. At that time, the authors attributed this to improved mass transport properties of the catalyst layer due to the loss of inactive species [7]. In order to deeply understand this phenomenon, which is different from the phenomenon of the instability of Fe-based catalysts in acid media reported in previous work [106], they performed further research on the stability of iron species in heat-treated Fe-based catalysts by combining the X-ray absorption near-edge structure (XANES) spectra edge-step analysis and inductively-coupled mass spectrometry measurement with the results of electrochemical measurement [105]. The results obtained by the authors show that Fe was lost from the Fe-based catalyst into the electrochemical environment during the ORR process in acid medium and the kinetic losses of ORR catalytic activity may be attribute to the oxidation of active sites and/or loss of pyridinic-like and pyrrolic-like Fe coordination (Fe–N<sub>2</sub> and Fe–N<sub>4</sub>), as well as the mass transport improvement due to the removal of inactive Fe species, predominantly sulfides (FeS and FeS<sub>2</sub>), while the durability of this Fe-based catalysts is depend on the stability of the porphyrin-like Fe coordination [105]. This report elucidates a clear relationship between the electrocatalytic ORR activity and stability of Fe-based catalysts and the Fe species, which has a major significance for designing and preparing the highly stable Fe-base ORR catalysts.

In this section, we may safely draw the conclusion that great progress has been made in exploration of ORR active sites formation mechanisms, structure and stability. Fe-centered active sites possess a unique structure and exhibit very high catalytic activity for ORR, and will show an important role in the development of high-performance Fe-based catalysts. It is worth notice that the Fe-based catalysts synthesized by ACTA S. P. A (An Italy-based company engaged in the development, production and marketing of clean technology products for fuel cells and other hydrogen applications) show outstanding electrochemical ORR performance in alkaline media with a maximum power density of 120 mW cm<sup>-2</sup> during the direct methanol fuel cell test, which show an important progress in the commercialization of fuel cell and attracting significant interest from several groups with alkaline fuel cell chemistry [107,108]. A long way, however, is still needed in order to reach the practical usage of Fe-based catalysts in the acid system of fuel cells applications. The exact role of the iron-ion center regarding the ORR active site as well as the structures of the active site should be investigated in detail in order to provide further insight into this topic.

### 3. Conclusions and Perspectives

The current Pt and Pt-based alloy electron catalysts, although they exhibit good ORR activities, suffer from many application challenges, such as high cost and weak durability. Meanwhile, a great advantage of recently developed Fe/N/C electrocatalysts (Fe-based catalysts) is their competitive ORR performance compared with Pt-based materials. Based on the previous report by Zhang *et al.*, this review paper focuses on the progress in this research field over the recent five years. Compared to high-temperature pyrolysis of iron N<sub>4</sub> chelate complexes, Fe-based materials prepared by the simple pyrolysis of transition metal salt carbon support, and nitrogen-rich small molecule polymeric compound are mainly reviewed due to their low cost, high performance, long stability and most

promising for replace currently used Pt-based catalysts in the progress of fuel cell commercialization. Additionally, Fe-base catalysts are presented to analyze the effect of Fe loading and existence form on the ORR catalytic activity in Fe-base catalyst. The proposed Fe-centered active sites and reaction mechanisms from various authors are also discussed in detail, which may be of importance for rational designing of high-performance, inexpensive, and practical Fe-base ORR catalysts in future development of fuel cells.

Numerous types of Fe-based ORR catalysts have been developed with ORR catalytic activity comparable with or better than Pt; however, almost all of them only show high catalytic activity in alkaline medium rather than in acidic condition. Due to the limitations of alkaline fuel cells, the acidic fuel cells are more popular. So, in the future research directions, developing of Fe-based catalysts with catalytic activity as highly as that of Pt in acidic condition is more urgent. In order to solve this problem, further study on the catalytic mechanism and kinetics is still needed in order to design and develop rationally carbon-based, Fe-based catalysts with a desirable activity and durability, especially in acidic conditions.

For the final industrial or commercial application, it is also essential to develop simple and cost-efficient methods for the large-scale production of Fe-based catalysts with excellent ORR electrocatalytic activity and long-term operation stability.

### Acknowledgments

This work was funded by National Basic Research Program of China (973 Program, 2014CB932700, 2012CB932800 and 2012CB215500), National Natural Science Foundation of China (21273220, 21303180 and 21422307), and “the Recruitment Program of Global youth Experts” of China.

### Author Contributions

Jing Liu wrote the most parts of the article, Erling Li contributed to the revise of the review in later stage, Mingbo Ruan and Ping Song were responsible for the mechanism in the article, Weilin Xu checked the article in the process of writing and modification.

### Conflicts of Interest

The authors declare no conflict of interest.

### References

1. Steele, B.C.H.; Heinzel, A. Materials for fuel-cell technologies. *Nature* **2001**, *414*, 345–352.
2. Higgins, D.; Chen, Z. Recent Development of Non-precious Metal Catalysts. In *Lecture Notes in Energy—Electrocatalysis in Fuel Cells*; Shao, M., Ed.; Springer: New York, NY, USA, 2013; Volume 9, pp. 247–270.
3. Gasteiger, H.A.; Kocha, S.S.; Sompalli, B.; Wagner, F.T. Activity benchmarks and requirements for Pt, Pt-alloy, and non-Pt oxygen reduction catalysts for PEMFCs. *Appl. Catal. B* **2005**, *56*, 9–35.

4. Borup, R.; Meyers, J.; Pivovar, B.; Kim, Y.S.; Mukundan, R.; Garland, N.; Myers, D.; Wilson, M.; Garzon, F.; Wood, D.; *et al.* Scientific Aspects of Polymer Electrolyte Fuel Cell Durability and Degradation. *Chem. Rev.* **2007**, *107*, 3904–3951.
5. Jasinski, R. A New Fuel Cell Cathode Catalyst. *Nature* **1964**, *201*, 1212–1213.
6. Jeon, I.-Y.; Choi, H.-J.; Choi, M.; Seo, J.-M.; Jung, S.-M.; Kim, M.-J.; Zhang, S.; Zhang, L.; Xia, Z.; Dai, L.; *et al.* Facile, scalable synthesis of edge-halogenated graphenenanoplatelets as efficient metal-free electrocatalysts for oxygen reduction reaction. *Sci. Rep.* **2013**, *3*, doi:10.1038/srep01810.
7. Wu, G.; More, K.L.; Johnston, C.M.; Zelenay, P. High-Performance Electrocatalysts for Oxygen Reduction Derived from Polyaniline, Iron, and Cobalt. *Science* **2011**, *332*, 443–447.
8. Gong, K.; Du, F.; Xia, Z.; Durstock, M.; Dai, L. Nitrogen-Doped Carbon Nanotube Arrays with High Electrocatalytic Activity for Oxygen Reduction. *Science* **2009**, *323*, 760–764.
9. Sun, X.; Zhang, Y.; Song, P.; Pan, J.; Zhuang, L.; Xu, W.; Xing, W. Fluorine-Doped Carbon Blacks: Highly Efficient Metal-Free Electrocatalysts for Oxygen Reduction Reaction. *ACS Catal.* **2013**, *3*, 1726–1729.
10. Sun, X.; Song, P.; Zhang, Y.; Liu, C.; Xu, W.; Xing, W. A Class of High Performance Metal-Free Oxygen Reduction Electrocatalysts based on Cheap Carbon Blacks. *Sci. Rep.* **2013**, *3*, doi:10.1038/srep02505.
11. Oh, H.-S.; Kim, H. The role of transition metals in non-precious nitrogen-modified carbon-based electrocatalysts for oxygen reduction reaction. *J. Power Sources* **2012**, *212*, 220–225.
12. Jaouen, F. Heat-Treated Transition Metal-N<sub>x</sub>C<sub>y</sub> Electrocatalysts for the O<sub>2</sub> Reduction Reaction in Acid PEM Fuel Cells. In *Non-Noble Metal Fuel Cell Catalysts*; Wiley-VCH Verlag GmbH & Co. KGaA: Weinheim, Germany, 2014; pp. 29–118.
13. Chen, Z.; Higgins, D.; Yu, A.; Zhang, L.; Zhang, J. A review on non-precious metal electrocatalysts for PEM fuel cells. *Energy Environ. Sci.* **2011**, *4*, 3167–3192.
14. Jaouen, F.; Proietti, E.; Lefèvre, M.; Chenitz, R.; Dodelet, J.-P.; Wu, G.; Chung, H.T.; Johnston, C.M.; Zelenay, P. Recent advances in non-precious metal catalysis for oxygen-reduction reaction in polymer electrolyte fuel cells. *Energy Environ. Sci.* **2011**, *4*, 114–130.
15. Xiang, Z.; Xue, Y.; Cao, D.; Huang, L.; Chen, J.-F.; Dai, L. Highly Efficient Electrocatalysts for Oxygen Reduction Based on 2D Covalent Organic Polymers Complexed with Non-precious Metals. *Angew. Chem. Int. Ed.* **2014**, *53*, 2433–2437.
16. Koslowski, U.I.; Abs-Wurmbach, I.; Fiechter, S.; Bogdanoff, P. Nature of the Catalytic Centers of Porphyrin-Based Electrocatalysts for the ORR: A Correlation of Kinetic Current Density with the Site Density of Fe–N<sub>4</sub> Centers. *J. Phys. Chem. C* **2008**, *112*, 15356–15366.
17. Bouwkamp-Wijnoltz, A.L.; Visscher, W.; van Veen, J.A.R.; Boellaard, E.; van der Kraan, A.M.; Tang, S.C. On Active-Site Heterogeneity in Pyrolyzed Carbon-Supported Iron Porphyrin Catalysts for the Electrochemical Reduction of Oxygen: An *In Situ* Mössbauer Study. *J. Phys. Chem. B* **2002**, *106*, 12993–13001.
18. Bae, I.T.; Tryk, D.A.; Scherson, D.A. Effect of Heat Treatment on the Redox Properties of Iron Porphyrins Adsorbed on High Area Carbon in Acid Electrolytes: An *In Situ* Fe K-Edge X-ray Absorption Near-Edge Structure Study. *J. Phys. Chem. B* **1998**, *102*, 4114–4117.

19. Schulenburg, H.; Stankov, S.; Schünemann, V.; Radnik, J.; Dorbandt, I.; Fiechter, S.; Bogdanoff, P.; Tributsch, H. Catalysts for the Oxygen Reduction from Heat-Treated Iron(III) Tetramethoxyphenylporphyrin Chloride: Structure and Stability of Active Sites. *J. Phys. Chem.* **2003**, *107*, 9034–9041.
20. Arechederra, R.L.; Artyushkova, K.; Atanassov, P.; Minteer, S.D. Growth of Phthalocyanine Doped and Undoped Nanotubes Using Mild Synthesis Conditions for Development of Novel Oxygen Reduction Catalysts. *ACS Appl. Mater. Interfaces* **2010**, *2*, 3295–3302.
21. Rigsby, M.L.; Wasylenko, D.J.; Pegis, M.L.; Mayer, J.M. Medium Effects Are as Important as Catalyst Design for Selectivity in Electrocatalytic Oxygen Reduction by Iron-Porphyrin Complexes. *J. Am. Chem. Soc.* **2015**, *137*, 4296–4299.
22. Bezerra, C.W.B.; Zhang, L.; Lee, K.; Liu, H.; Zhang, J.; Shi, Z.; Marques, A.L.B.; Marques, E.P.; Wu, S.; Zhang, J. Novel carbon-supported Fe–N electrocatalysts synthesized through heat treatment of iron tripyridyltriazine complexes for the PEM fuel cell oxygen reduction reaction. *Electrochim. Acta* **2008**, *53*, 7703–7710.
23. Liu, H.; Shi, Z.; Zhang, J.; Zhang, L.; Zhang, J. Ultrasonic spray pyrolyzed iron-polypyrrole mesoporous spheres for fuel celloxygen reduction electrocatalysts. *J. Mater. Chem.* **2009**, *19*, 468–470.
24. Choi, J.-Y.; Higgins, D.; Chen, Z. Highly Durable GrapheneNanosheet Supported Iron Catalyst for Oxygen Reduction Reaction in PEM Fuel Cells. *J. Electrochem. Soc.* **2011**, *159*, B86–B89.
25. Ye, S.; Vijh, A.K. Non-noble metal-carbonized aerogel composites as electrocatalysts for the oxygen reduction reaction. *Electrochem. Commun.* **2003**, *5*, 272–275.
26. Lalande, G.; Côté, R.; Guay, D.; Dodelet, J.P.; Weng, L.T.; Bertrand, P. Is nitrogen important in the formulation of Fe-based catalysts for oxygen reduction in solid polymer fuel cells? *Electrochim. Acta* **1997**, *42*, 1379–1388.
27. Hsu, R.S.; Chen, Z. Improved Synthesis Method for a Cyanamide Derived Non-Precious ORR Catalyst for PEFCs. *ECS Trans.* **2010**, *28*, 39–46.
28. Choi, J.-Y.; Hsu, R.S.; Chen, Z. Highly Active Porous Carbon-Supported Nonprecious Metal-N Electrocatalyst for Oxygen Reduction Reaction in PEM Fuel Cells. *J. Phys. Chem. C* **2010**, *114*, 8048–8053.
29. Choi, J.-Y.; Hsu, R.S.; Chen, Z. Nanoporous Carbon-Supported Fe/Co–N Electrocatalyst for Oxygen Reduction Reaction in PEM Fuel Cells. *ECS Trans.* **2010**, *28*, 101–112.
30. Chung, H.T.; Johnston, C.M.; Artyushkova, K.; Ferrandon, M.; Myers, D.J.; Zelenay, P. Cyanamide-derived non-precious metal catalyst for oxygen reduction. *Electrochem. Commun.* **2010**, *12*, 1792–1795.
31. Jaouen, F.; Lefèvre, M.; Dodelet, J.-P.; Cai, M. Heat-Treated Fe/N/C Catalysts for O<sub>2</sub> Electroreduction: Are Active Sites Hosted in Micropores? *J. Phys. Chem. B* **2006**, *110*, 5553–5558.
32. Choi, C.H.; Park, S.H.; Woo, S.I. N-doped carbon prepared by pyrolysis of dicyandiamide with various MeCl<sub>2</sub>·xH<sub>2</sub>O (Me = Co, Fe, and Ni) composites: Effect of type and amount of metal seed on oxygen reduction reactions. *Appl. Catal. B* **2012**, *119–120*, 123–131.

33. Tian, J.; Morozan, A.; Sougrati, M.T.; Lefèvre, M.; Chenitz, R.; Dodelet, J.-P.; Jones, D.; Jaouen, F. Optimized Synthesis of Fe/N/C Cathode Catalysts for PEM Fuel Cells: A Matter of Iron-Ligand Coordination Strength. *Angew. Chem. Int. Ed.* **2013**, *52*, 6867–6870.
34. Wang, M.-Q.; Yang, W.-H.; Wang, H.-H.; Chen, C.; Zhou, Z.-Y.; Sun, S.-G. Pyrolyzed Fe–N–C Composite as an Efficient Non-precious Metal Catalyst for Oxygen Reduction Reaction in Acidic Medium. *ACS Catal.* **2014**, *4*, 3928–3936.
35. Lefèvre, M.; Dodelet, J.P.; Bertrand, P. O<sub>2</sub> Reduction in PEM Fuel Cells: Activity and Active Site Structural Information for Catalysts Obtained by the Pyrolysis at High Temperature of Fe Precursors. *J. Phys. Chem. B* **2000**, *104*, 11238–11247.
36. Liu, J.; Sun, X.; Song, P.; Zhang, Y.; Xing, W.; Xu, W. High-Performance Oxygen Reduction Electrocatalysts based on Cheap Carbon Black, Nitrogen, and Trace Iron. *Adv. Mater.* **2013**, *25*, 6879–6883.
37. Li, X.; Liu, G.; Popov, B.N. Activity and stability of non-precious metal catalysts for oxygen reduction in acid and alkaline electrolytes. *J. Power Sources* **2010**, *195*, 6373–6378.
38. Jiang, Y.; Lu, Y.; Lv, X.; Han, D.; Zhang, Q.; Niu, L.; Chen, W. Enhanced Catalytic Performance of Pt-Free Iron Phthalocyanine by Graphene Support for Efficient Oxygen Reduction Reaction. *ACS Catal.* **2013**, *3*, 1263–1271.
39. Xiao, M.; Zhu, J.; Feng, L.; Liu, C.; Xing, W. Meso/Macroporous Nitrogen-Doped Carbon Architectures with Iron Carbide Encapsulated in Graphitic Layers as an Efficient and Robust Catalyst for the Oxygen Reduction Reaction in Both Acidic and Alkaline Solutions. *Adv. Mater.* **2015**, *27*, 2521–2527.
40. Niu, W.; Li, L.; Liu, X.; Wang, N.; Liu, J.; Zhou, W.; Tang, Z.; Chen, S. Mesoporous N-Doped Carbons Prepared with Thermally Removable Nanoparticle Templates: An Efficient Electrocatalyst for Oxygen Reduction Reaction. *J. Am. Chem. Soc.* **2015**, *137*, 5555–5562.
41. Wang, Q.; Zhou, Z.-Y.; Lai, Y.-J.; You, Y.; Liu, J.-G.; Wu, X.-L.; Terefe, E.; Chen, C.; Song, L.; Rauf, M.; *et al.* Phenylenediamine-Based FeN<sub>x</sub>/C Catalyst with High Activity for Oxygen Reduction in Acid Medium and Its Active-Site Probing. *J. Am. Chem. Soc.* **2014**, *136*, 10882–10885.
42. Yin, J.; Qiu, Y.; Yu, J. Onion-like graphitic nanoshell structured Fe–N/C nanofibers derived from electrospinning for oxygen reduction reaction in acid media. *Electrochem. Commun.* **2013**, *30*, 1–4.
43. Li, Y.; Zhou, W.; Wang, H.; Xie, L.; Liang, Y.; Wei, F.; Idrobo, J.-C.; Pennycook, S.J.; Dai, H. An oxygen reduction electrocatalyst based on carbon nanotube-graphene complexes. *Nat. Nanotechnol.* **2012**, *7*, 394–400.
44. Kramm, U.I.; Herranz, J.; Larouche, N.; Arruda, T.M.; Lefevre, M.; Jaouen, F.; Bogdanoff, P.; Fiechter, S.; Abs-Wurmbach, I.; Mukerjee, S.; *et al.* Structure of the catalytic sites in Fe/N/C-catalysts for O<sub>2</sub>-reduction in PEM fuel cells. *Phys. Chem. Chem. Phys.* **2012**, *14*, 11673–11688.
45. Li, W.; Wu, J.; Higgins, D.C.; Choi, J.-Y.; Chen, Z. Determination of Iron Active Sites in Pyrolyzed Iron-Based Catalysts for the Oxygen Reduction Reaction. *ACS Catal.* **2012**, *2*, 2761–2768.

46. Singh, D.; Mamtani, K.; Bruening, C.R.; Miller, J.T.; Ozkan, U.S. Use of H<sub>2</sub>S to Probe the Active Sites in FeNC Catalysts for the Oxygen Reduction Reaction (ORR) in Acidic Media. *ACS Catal.* **2014**, *4*, 3454–3462.
47. Zhu, Y.; Zhang, B.; Liu, X.; Wang, D.-W.; Su, D.S. Unravelling the Structure of Electrocatalytically Active Fe–N Complexes in Carbon for the Oxygen Reduction Reaction. *Angew. Chem. Int. Ed.* **2014**, *53*, 10673–10677.
48. Tylus, U.; Jia, Q.; Strickland, K.; Ramaswamy, N.; Serov, A.; Atanassov, P.; Mukerjee, S. Elucidating Oxygen Reduction Active Sites in Pyrolyzed Metal-Nitrogen Coordinated Non-Precious-Metal Electrocatalyst Systems. *J. Phys. Chem. C* **2014**, *118*, 8999–9008.
49. Robson, M.H.; Serov, A.; Artyushkova, K.; Atanassov, P. A mechanistic study of 4-aminoantipyrine and iron derived non-platinum group metal catalyst on the oxygen reduction reaction. *Electrochim. Acta* **2013**, *90*, 656–665.
50. Kattel, S.; Wang, G. A density functional theory study of oxygen reduction reaction on Me–N<sub>4</sub> (Me = Fe, Co, or Ni) clusters between graphitic pores. *J. Mater. Chem. A* **2013**, *1*, 10790–10797.
51. Badger, G.; Jones, R.; Laslett, R. Porphyrins. VII. The synthesis of porphyrins by the Rothmund reaction. *Aust. J. Chem.* **1964**, *17*, 1028–1035.
52. Baranton, S.; Coutanceau, C.; Roux, C.; Hahn, F.; Léger, J.M. Oxygen reduction reaction in acid medium at iron phthalocyanine dispersed on high surface area carbon substrate: Tolerance to methanol, stability and kinetics. *J. Electroanal. Chem.* **2005**, *577*, 223–234.
53. Vasudevan, P.; Satya, S. Mann, N.; Tyagi, S. Transition metal complexes of porphyrins and phthalocyanines as electrocatalysts for dioxygen reduction. *Transit. Met. Chem.* **1990**, *15*, 81–90.
54. Zagal, J.H. Metallophthalocyanines as catalysts in electrochemical reactions. *Coord. Chem. Rev.* **1992**, *119*, 89–136.
55. Morozan, A.; Campidelli, S.; Filoramo, A.; Jusselme, B.; Palacin, S. Catalytic activity of cobalt and iron phthalocyanines or porphyrins supported on different carbon nanotubes towards oxygen reduction reaction. *Carbon* **2011**, *49*, 4839–4847.
56. Faubert, G.; Lalande, G.; Côté, R.; Guay, D.; Dodelet, J.P.; Weng, L.T.; Bertrand, P.; Dénès, G. Heat-treated iron and cobalt tetraphenylporphyrins adsorbed on carbon black: Physical characterization and catalytic properties of these materials for the reduction of oxygen in polymer electrolyte fuel cells. *Electrochim. Acta* **1996**, *41*, 1689–1701.
57. Gupta, S.; Tryk, D.; Bae, I.; Aldred, W.; Yeager, E. Heat-treated polyacrylonitrile-based catalysts for oxygen electroreduction. *J. Appl. Electrochem.* **1989**, *19*, 19–27.
58. Wu, G.; Chen, Z.; Artyushkova, K.; Garzon, F.H.; Zelenay, P. Polyaniline-derived Non-Precious Catalyst for the Polymer Electrolyte Fuel Cell Cathode. *ECS Trans.* **2008**, *16*, 159–170.
59. Kramm, U.I.; Abs-Wurmbach, I.; Herrmann-Geppert, I.; Radnik, J.; Fiechter, S.; Bogdanoff, P. Influence of the Electron-Density of FeN<sub>4</sub>-Centers Towards the Catalytic Activity of Pyrolyzed FeTMPPCl-Based ORR-Electrocatalysts. *J. Electrochem. Soc.* **2011**, *158*, B69–B78.
60. Lefèvre, M.; Dodelet, J.P.; Bertrand, P. Molecular Oxygen Reduction in PEM Fuel Cells: Evidence for the Simultaneous Presence of Two Active Sites in Fe-Based Catalysts. *J. Phys. Chem. B* **2002**, *106*, 8705–8713.

61. Charretre, F.; Jaouen, F.; Ruggeri, S.; Dodelet, J.-P. Fe/N/C non-precious catalysts for PEM fuel cells: Influence of the structural parameters of pristine commercial carbon blacks on their activity for oxygen reduction. *Electrochim. Acta* **2008**, *53*, 2925–2938.
62. Liu, G.; Li, X.; Ganesan, P.; Popov, B.N. Studies of oxygen reduction reaction active sites and stability of nitrogen-modified carbon composite catalysts for PEM fuel cells. *Electrochim. Acta* **2010**, *55*, 2853–2858.
63. Nabae, Y.; Moriya, S.; Matsubayashi, K.; Lyth, S.M.; Malon, M.; Wu, L.; Islam, N.M.; Koshigoe, Y.; Kuroki, S.; Kakimoto, M.-A.; *et al.* RETRACTED: The role of Fe species in the pyrolysis of Fe phthalocyanine and phenolic resin for preparation of carbon-based cathode catalysts. *Carbon* **2010**, *48*, 2613–2624.
64. Baker, R.; Wilkinson, D.P.; Zhang, J. Electrocatalytic activity and stability of substituted iron phthalocyanines towards oxygen reduction evaluated at different temperatures. *Electrochim. Acta* **2008**, *53*, 6906–6919.
65. Li, W.; Yu, A.; Higgins, D.C.; Llanos, B.G.; Chen, Z. Biologically Inspired Highly Durable Iron Phthalocyanine Catalysts for Oxygen Reduction Reaction in Polymer Electrolyte Membrane Fuel Cells. *J. Am. Chem. Soc.* **2010**, *132*, 17056–17058.
66. Liu, G.; Li, X.; Ganesan, P.; Popov, B.N. Development of non-precious metal oxygen-reduction catalysts for PEM fuel cells based on N-doped ordered porous carbon. *Appl. Catal. B* **2009**, *93*, 156–165.
67. Velázquez-Palenzuela, A.; Zhang, L.; Wang, L.; Cabot, P.L.; Brillas, E.; Tsay, K.; Zhang, J. Carbon-Supported Fe–N<sub>x</sub> Catalysts Synthesized by Pyrolysis of the Fe(II)–2,3,5,6-Tetra(2-pyridyl)pyrazine Complex: Structure, Electrochemical Properties, and Oxygen Reduction Reaction Activity. *J. Phys. Chem. C* **2011**, *115*, 12929–12940.
68. Zhang, L.; Lee, K.; Bezerra, C.W.B.; Zhang, J.; Zhang, J. Fe loading of a carbon-supported Fe–N electrocatalyst and its effect on the oxygen reduction reaction. *Electrochim. Acta* **2009**, *54*, 6631–6636.
69. Jaouen, F.; Marcotte, S.; Dodelet, J.-P.; Lindbergh, G. Oxygen Reduction Catalysts for Polymer Electrolyte Fuel Cells from the Pyrolysis of Iron Acetate Adsorbed on Various Carbon Supports. *J. Phys. Chem. B* **2003**, *107*, 1376–1386.
70. Nallathambi, V.; Lee, J.-W.; Kumaraguru, S.P.; Wu, G.; Popov, B.N. Development of high performance carbon composite catalyst for oxygen reduction reaction in PEM Proton Exchange Membrane fuel cells. *J. Power Sources* **2008**, *183*, 34–42.
71. Lefevre, M.; Proietti, E.; Jaouen, F.; Dodelet, J.P. Iron-Based Catalysts with Improved Oxygen Reduction Activity in Polymer Electrolyte Fuel Cells. *Science* **2009**, *324*, 71–74.
72. Proietti, E.; Jaouen, F.; Lefèvre, M.; Larouche, N.; Tian, J.; Herranz, J.; Dodelet, J.-P. Iron-based cathode catalyst with enhanced power density in polymer electrolyte membrane fuel cells. *Nat. Commun.* **2011**, *2*, 416.
73. Kramm, U.I.; Lefèvre, M.; Larouche, N.; Schmeisser, D.; Dodelet, J.-P. Correlations between Mass Activity and Physicochemical Properties of Fe/N/C Catalysts for the ORR in PEM Fuel Cell via <sup>57</sup>Fe Mössbauer Spectroscopy and Other Techniques. *J. Am. Chem. Soc.* **2014**, *136*, 978–985.

74. Byon, H.R.; Suntivich, J.; Shao-Horn, Y. Graphene-Based Non-Noble-Metal Catalysts for Oxygen Reduction Reaction in Acid. *Chem. Mater.* **2011**, *23*, 3421–3428.
75. Wu, G.; Johnston, C.M.; Mack, N.H.; Artyushkova, K.; Ferrandon, M.; Nelson, M.; Lezama-Pacheco, J.S.; Conradson, S.D.; More, K.L.; Myers, D.J.; *et al.* Synthesis-structure-performance correlation for polyaniline-Me-C non-precious metal cathode catalysts for oxygen reduction in fuel cells. *J. Mater. Chem.* **2011**, *21*, 11392–11405.
76. Wu, G.; Nelson, M.; Ma, S.; Meng, H.; Cui, G.; Shen, P.K. Synthesis of nitrogen-doped onion-like carbon and its use in carbon-based CoFe binary non-precious-metal catalysts for oxygen-reduction. *Carbon* **2011**, *49*, 3972–3982.
77. Jahan, M.; Bao, Q.; Loh, K.P. Electrocatalytically Active Graphene-Porphyrin MOF Composite for Oxygen Reduction Reaction. *J. Am. Chem. Soc.* **2012**, *134*, 6707–6713.
78. Yang, T.; Han, G. Synthesis of a Novel Catalyst via Pyrolyzing Melamine with Fe Precursor and its Excellent Electrocatalysis for Oxygen Reduction. *Int. J. Electrochem. Sci.* **2012**, *7*, 10884–10893.
79. Xiao, H.; Shao, Z.-G.; Zhang, G.; Gao, Y.; Lu, W.; Yi, B. Fe–N–carbon black for the oxygen reduction reaction in sulfuric acid. *Carbon* **2013**, *57*, 443–451.
80. Lopes, T.; Olivi, P. Non-precious Metal Oxygen Reduction Reaction Catalysts Synthesized via Cyanuric Chloride and *N*-Ethylamine. *Electrocatalysis* **2014**, *5*, 396–401.
81. Qiu, Y.; Yu, J.; Wu, W.; Yin, J.; Bai, X. Fe–N/C nanofiber electrocatalysts with improved activity and stability for oxygen reduction in alkaline and acid solutions. *J. Solid State Electrochem.* **2012**, *17*, 565–573.
82. Serov, A.; Robson, M.H.; Artyushkova, K.; Atanassov, P. Templated non-PGM cathode catalysts derived from iron and poly(ethyleneimine) precursors. *Appl. Catal. B* **2012**, *127*, 300–306.
83. Serov, A.; Robson, M.H.; Halevi, B.; Artyushkova, K.; Atanassov, P. Highly active and durable templated non-PGM cathode catalysts derived from iron and aminoantipyrine. *Electrochem. Commun.* **2012**, *22*, 53–56.
84. Serov, A.; Robson, M.H.; Smolnik, M.; Atanassov, P. Tri-metallic transition metal-nitrogen-carbon catalysts derived by sacrificial support method synthesis. *Electrochim. Acta* **2013**, *109*, 433–439.
85. Nallathambi, V.; Leonard, N.; Kothandaraman, R.; Barton, S.C. Nitrogen Precursor Effects in Iron-Nitrogen-Carbon Oxygen Reduction Catalysts. *Electrochem. Solid-State Lett.* **2011**, *14*, B55–B58.
86. Wu, Z.-S.; Yang, S.; Sun, Y.; Parvez, K.; Feng, X.; Müllen, K. 3D Nitrogen-Doped Graphene Aerogel-Supported Fe<sub>3</sub>O<sub>4</sub> Nanoparticles as Efficient Electrocatalysts for the Oxygen Reduction Reaction. *J. Am. Chem. Soc.* **2012**, *134*, 9082–9085.
87. Chung, H.T.; Won, J.H.; Zelenay, P. Active and stable carbon nanotube/nanoparticle composite electrocatalyst for oxygen reduction. *Nat. Commun.* **2013**, *4*, 1922.
88. Kim, B.J.; Lee, D.U.; Wu, J.; Higgins, D.; Yu, A.; Chen, Z. Iron- and Nitrogen-Functionalized Graphene Nanosheet and Nanoshell Composites as a Highly Active Electrocatalyst for Oxygen Reduction Reaction. *J. Phys. Chem. C* **2013**, *117*, 26501–26508.
89. Zhang, S.; Liu, B.; Chen, S. Synergistic increase of oxygen reduction favourable Fe–N coordination structures in a ternary hybrid of carbon nanospheres/carbon nanotubes/graphene sheets. *Phys. Chem. Chem. Phys.* **2013**, *15*, 18482–18490.

90. Mo, Z.; Peng, H.; Liang, H.; Liao, S. Vesicular nitrogen doped carbon material derived from Fe<sub>2</sub>O<sub>3</sub> templated polyaniline as improved non-platinum fuel cell cathode catalyst. *Electrochim. Acta* **2013**, *99*, 30–37.
91. Cao, R.; Thapa, R.; Kim, H.; Xu, X.; Gyu Kim, M.; Li, Q.; Park, N.; Liu, M.; Cho, J. Promotion of oxygen reduction by a bio-inspired tethered iron phthalocyanine carbon nanotube-based catalyst. *Nat. Commun.* **2013**, *4*, 2076.
92. Zhao, D.; Shui, J.-L.; Grabstanowicz, L.R.; Chen, C.; Commet, S.M.; Xu, T.; Lu, J.; Liu, D.-J. Electrocatalysts: Highly Efficient Non-Precious Metal Electrocatalysts Prepared from One-Pot Synthesized Zeolitic Imidazolate Frameworks. *Adv. Mater.* **2014**, *26*, 1093–1097.
93. Yuan, S.; Shui, J.-L.; Grabstanowicz, L.; Chen, C.; Commet, S.; Reprögle, B.; Xu, T.; Yu, L.; Liu, D.-J. A Highly Active and Support-Free Oxygen Reduction Catalyst Prepared from Ultrahigh-Surface-Area Porous Polyporphyrin. *Angew. Chem. Int. Ed.* **2013**, *52*, 8349–8353.
94. Wen, Z.; Ci, S.; Zhang, F.; Feng, X.; Cui, S.; Mao, S.; Luo, S.; He, Z.; Chen, J. Nitrogen-Enriched Core-Shell Structured Fe/Fe<sub>3</sub>C-C Nanorods as Advanced Electrocatalysts for Oxygen Reduction Reaction. *Adv. Mater.* **2012**, *24*, 1399–1404.
95. Deng, D.; Yu, L.; Chen, X.; Wang, G.; Jin, L.; Pan, X.; Deng, J.; Sun, G.; Bao, X. Iron Encapsulated within Pod-like Carbon Nanotubes for Oxygen Reduction Reaction. *Angew. Chem. Int. Ed.* **2013**, *52*, 371–375.
96. Lee, J.-S.; Park, G.S.; Kim, S.T.; Liu, M.; Cho, J. A Highly Efficient Electrocatalyst for the Oxygen Reduction Reaction: N-Doped Ketjenblack Incorporated into Fe/Fe<sub>3</sub>C-Functionalized Melamine Foam. *Angew. Chem. Int. Ed.* **2013**, *52*, 1026–1030.
97. Hu, Y.; Jensen, J.O.; Zhang, W.; Cleemann, L.N.; Xing, W.; Bjerrum, N.J.; Li, Q. Hollow Spheres of Iron Carbide Nanoparticles Encased in Graphitic Layers as Oxygen Reduction Catalysts. *Angew. Chem. Int. Ed.* **2014**, *53*, 3675–3679.
98. Peng, H.; Liu, F.; Liu, X.; Liao, S.; You, C.; Tian, X.; Nan, H.; Luo, F.; Song, H.; Fu, Z.; *et al.* Effect of Transition Metals on the Structure and Performance of the Doped Carbon Catalysts Derived From Polyaniline and Melamine for ORR Application. *ACS Catal.* **2014**, *4*, 3797–3805.
99. Wang, L.; Ambrosi, A.; Pumera, M. “Metal-Free” Catalytic Oxygen Reduction Reaction on Heteroatom-Doped Graphene is Caused by Trace Metal Impurities. *Angew. Chem. Int. Ed.* **2013**, *52*, 13818–13821.
100. Jaouen, F.; Herranz, J.; Lefèvre, M.; Dodelet, J.-P.; Kramm, U.I.; Herrmann, I.; Bogdanoff, P.; Maruyama, J.; Nagaoka, T.; Garsuch, A.; *et al.* Cross-Laboratory Experimental Study of Non-Noble-Metal Electrocatalysts for the Oxygen Reduction Reaction. *ACS Appl. Mater. Interfaces* **2009**, *1*, 1623–1639.
101. Herranz, J.; Jaouen, F.; Lefèvre, M.; Kramm, U.I.; Proietti, E.; Dodelet, J.-P.; Bogdanoff, P.; Fiechter, S.; Abs-Wurmbach, I.; Bertrand, P.; *et al.* Unveiling N-Protonation and Anion-Binding Effects on Fe/N/C Catalysts for O<sub>2</sub> Reduction in Proton-Exchange-Membrane Fuel Cells. *J. Phys. Chem. C* **2011**, *115*, 16087–16097.
102. Carver, C.T.; Matson, B.D.; Mayer, J.M. Electrocatalytic Oxygen Reduction by Iron Tetra-arylporphyrins Bearing Pendant Proton Relays. *J. Am. Chem. Soc.* **2012**, *134*, 5444–5447.

103. Matson, B.D.; Carver, C.T.; von Ruden, A.; Yang, J.Y.; Raugei, S.; Mayer, J.M. Distant protonated pyridine groups in water-soluble iron porphyrin electrocatalysts promote selective oxygen reduction to water. *Chem. Commun.* **2012**, *48*, 11100–11102.
104. Ramaswamy, N.; Tylus, U.; Jia, Q.; Mukerjee, S. Activity Descriptor Identification for Oxygen Reduction on Nonprecious Electrocatalysts: Linking Surface Science to Coordination Chemistry. *J. Am. Chem. Soc.* **2013**, *135*, 15443–15449.
105. Ferrandon, M.; Wang, X.; Kropf, A.J.; Myers, D.J.; Wu, G.; Johnston, C.M.; Zelenay, P. Stability of iron species in heat-treated polyaniline-iron-carbon polymer electrolyte fuel cell cathode catalysts. *Electrochim. Acta* **2013**, *110*, 282–291.
106. Wu, G.; Artyushkova, K.; Ferrandon, M.; Kropf, A.J.; Myers, D.; Zelenay, P. Performance Durability of Polyaniline-derived Non-precious Cathode Catalysts. *ECS Trans.* **2009**, *25*, 1299–1311.
107. Varcoe, J.R.; Atanassov, P.; Dekel, D.R.; Herring, A.M.; Hickner, M.A.; Kohl, P.A.; Kucernak, A.R.; Mustain, W.E.; Nijmeijer, K.; Scott, K.; *et al.* Anion-exchange membranes in electrochemical energy systems. *Energy Environ. Sci.* **2014**, *7*, 3135–3191.
108. Katzfuß, A.; Poynton, S.; Varcoe, J.; Gogel, V.; Storr, U.; Kerres, J. Methylated polybenzimidazole and its application as a blend component in covalently cross-linked anion-exchange membranes for DMFC. *J. Membr. Sci.* **2014**, *465*, 129–137.

© 2015 by the authors; licensee MDPI, Basel, Switzerland. This article is an open access article distributed under the terms and conditions of the Creative Commons Attribution license (<http://creativecommons.org/licenses/by/4.0/>).